RESEARCH INVESTIGATIONS OF BULKHEAD CYLINDRICAL JUNCTIONS EXPOSED TO COMBINED LOAD, CRYOGENIC TEMPERATURE AND PRESSURE

PART III THEORETICAL ANALYSIS OF THE THERMAL LOADS

by

Chi-Wen Lin
C. A. Sciammarella
H. Wagner

Technical Report
Contract No. NAS8-5199
Prepared for
George C. Marshall Space Flight Center
NASA
Huntsville, Alabama
National Aeronautics and Space Administration
Washington 25, D. C.

Department of Engineering Science and Mechanics
Engineering and Industrial Experiment Station
University of Florida
Gainesville, Florida

August, 1964

RESEARCH INVESTIGATIONS OF BULKHEAD CYLINDRICAL JUNCTIONS EXPOSED TO COMBINED LOAD, CRYOGENIC TEMPERATURE PART III THEORETICAL ANALYSIS OF THE THERMAL LOADS

by

Chi-Wen Lin
C. A. Sciammarella
H. Wagner

Technical Report
Contract No. NAS8-5199
Prepared for
George C. Marshall Space Flight Center
NASA
Huntsville, Alabama
National Aeronautics and Space Administration
Washington 25, D. C.

Department of Engineering Science and Mechanics
Engineering and Industrial Experiment Station
University of Florida
Gainesville, Florida

August, 1964

TABLE OF CONTENTS

LIST OF FIGURES

ABSTRACT

26923

In the joint portion of the intertank of a missile, due to the varying thickness of each part of the shell, the low temperature fuel used in the tank and the comparative high temperature induced from the solar radiation may generate a highly polynomial distribution of the temperature at this region. The thermal stresses induced in this manner are important in considering the thin shell construction of the joint.

The problem is solved under the assumption of uniform temperature distribution along spatial axis of the cylindrical shell and constant in the whole semi-elliptical bulkhead. The temperature gradient in the axial axis is accepted from an experimental result but with modifications. Solution of this problem following an investigation based on the membrane theory leads to the fact of the existence of geometrical compatibility. The edge effects induced on considering the continuity of displacements and bending moment give the satisfactory solution for the present analysis. Author

CHAPTER I

INTRODUCTION

1.1 Preface

In the design of the intertank structures of missiles, the stresses and deformations are largely influenced by the thermal effect both from the low temperature fuel used and the comparatively high temperature caused by the solar radiation during the stage of fill, standby and flight. The construction of the intertank, consisting of a bulkhead and a cylindrical part connected with a skirt, is generally thin compared with the radius of curvature of the meridian of the shell. The edge effects of the various shell components produced by the abrupt change of the curvature and by the discontinuities in the mechanical loading, show that the joint portion (the so-called Y-ring) is the most important part in the design. The temperature gradient may have an important effect which is then of the same local character as the effect produced by the applied mechanical loads.

In the present analysis, the bulkhead has been taken as a semi-elliptical shell in revolution, and the intertank skirt is a corrugated skin cylindrical shell as shown in Figure 1. The temperature distribution, considered to be in the steady state and constant over the semi-elliptical bulkhead, has no spatial variation other than that in the longitudinal direction. An investigation based on the membrane theory has been worked out in Chapter II for the temperature indicated above, and

the problem has been solved for the proper boundary conditions. The solution of the edge effect is given in matrix form in Chapter III. However, no mathematical solutions for the influence coefficients have been derived, since it is understandable that such materials may be found in the books concerning problems of elastic foundations by M. Hetenyi [1]* and S. Timoshenko [2]. The numerical procedure in Chapter IV together with the discussion in Chapter V may present a better understanding of the entire problem in question.

We employ here three basic assumptions [3]; (1) The temperature is determined independently of the deformations of the body. (2) The deformations are small. (3) The materials behave elastically all the time. These items simply state that the coupling between the thermal field and the stress field may be omitted, that the displacement gradients are sufficiently small so that no buckling can take place in the present analysis, and finally, the temperature changes and the stresses will not be too large.

1.2 General sketch of the joint

The intertank, as described in the preface, consists of a bulkhead and a cylindrical part connected with a skirt. The bulkhead, which includes the cap portion with uniform thickness and the variable wall thickness knuckle part, is a semi-elliptical shell. The cylindrical part may be divided again into several sections. The numbers I, II, III, IV, V, VI, VII, and VIII have been used in the succeeding chapters representing the different parts in the following figure.

*Numbers in brackets denote entries in the List of References.

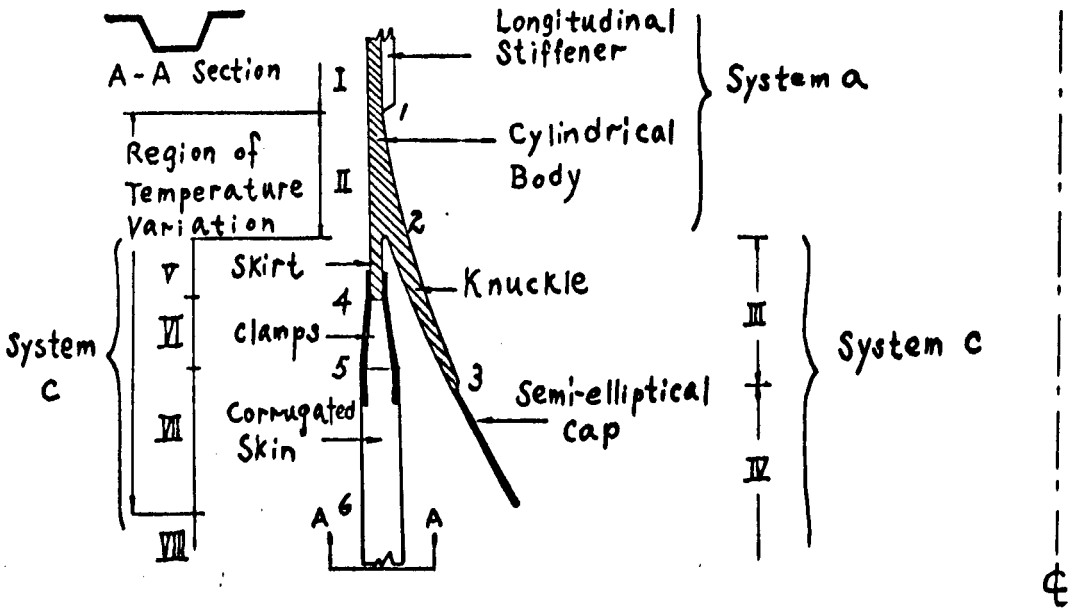

Fig. 1.--General sketch of the joint (Y-ring)

Fundamentally the entire process of solving the stresses problem for the intertank consists of three steps: (1) determination of the membrane stresses due to the temperature load, (2) determination of the stresses due to edge loads, (3) superposition.

CHAPTER II

MEMBRANE THEORY

2.1 Introduction

The general sketch in section 1.2 shows the geometrical configuration of the intertank. The thin shell construction together with the assumption of small deflection theory enables us to adopt the membrane theory as an analysis. For each of the different parts in Figure 1, the thermal stresses and displacements induced from the thermal loading, which is imposed by the longitudinal varying temperature distribution, may be obtained from the linearized membrane equations derived in the following sections. The arbitrary constants involved in the equations for each independent different part may be evaluated upon restoring the continuity of the parts investigated alone, and upon the imposing of the boundary conditions for the whole intertank.

2.2 Thermal stresses and displacements in a thin-walled circular cylindrical shell with non-uniform wall thickness and longitudinal temperature variation

The analysis of this section deals with the shell part II (see Figure 1) and also, as a special case of it, with the parts I and V.

Considering that the variation of temperature takes place only in the longitudinal direction and that the uniform expansion of the periphery is not subjected to any constraint under the thermal loading, and in as much as the shell remains cylindrical (c.f.2.3), only axial thermal stress can be induced.

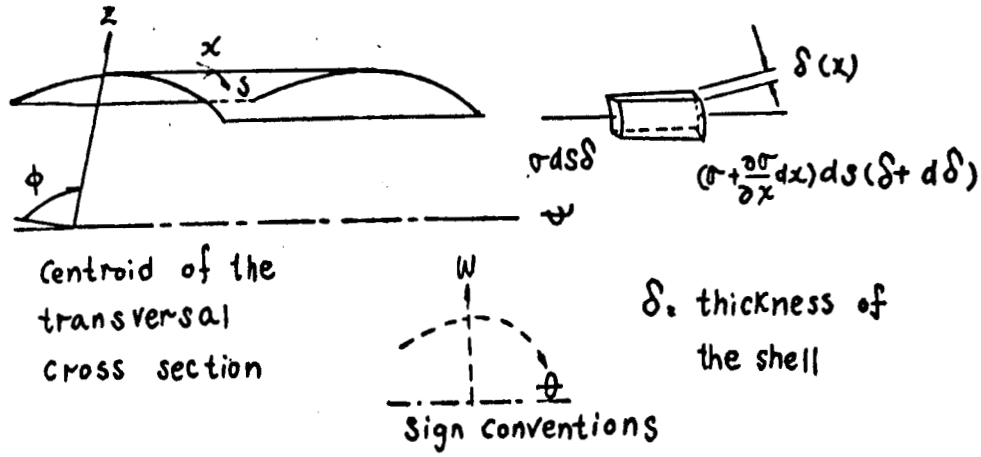

Fig. 2.--Coordinate system and general cylindrical element

A studying of a general cylindrical element shown in Figure 2 leads to the equilibrium condition in axial direction

$$\sigma d\delta + \frac{\partial \sigma}{\partial x} dx (\delta + d\delta) = 0 \tag{1}$$

neglecting the higher order term, it gives us

$$d(\delta\sigma) = 0 \tag{2}$$

that is

$$\delta\sigma = q_1 \tag{3}$$

δ and σ are both functions of x, whereas the integration constant q_1 may be determined by the boundary conditions imposed (see section 2.6).

We have the stress-strain relations 3

$$\varepsilon_{xx} = \frac{\partial u}{\partial x} = \frac{1}{E\delta(x)}\sigma + \alpha T \tag{4}_a$$

$$\varepsilon_{ss} = \frac{w}{R_o} = -\frac{\mu}{E\delta(x)}\sigma + \alpha T \tag{4}_b$$

$$\varepsilon_{xs} = \frac{\partial u}{\partial s} = 0 \tag{4}_c$$

Thereby it is understood that no displacements along the circumference may occur. Equation $(4)_b$ immediately leads to

$$W = -\frac{\mu R_0}{E\,\delta(x)}\sigma + \alpha T R_0 \tag{5}$$

and $(4)_a$ gives

$$U(x) = \int_0^x \frac{1}{E\,\delta(x)}\sigma\,dx + \int_0^x \alpha T\,dx + g_2 \,, \tag{6}$$

where g_2 may be an arbitrary function of λ; however, a close examination of $(4)_c$ reveals that it does not depend on λ. That is, g_2 is a constant.

By substituting equation (3) into equation (6) one obtains

$$U(x) = \frac{g_1}{E}\int_0^x \frac{1}{\delta(x)^2}\,dx + \alpha\int_0^x T\,dx + g_2 \tag{7}$$

Again, g_2 may be defined by the boundary conditions.

From (5), we have the slope of the shell in the axial direction in the present sign convention as

$$\theta = -\frac{dW}{dx} = -\left(\alpha R_0 \frac{dT}{dx}\right) + \frac{\mu R_0}{E}\frac{d}{dx}\left(\frac{\sigma}{\delta(x)}\right) \tag{8}$$

The second differentiation of W is

$$\frac{d^2W}{dx^2} = \alpha R_0 \frac{d^2T}{dx^2} - \frac{\mu R_0}{E}\frac{d^2}{dx^2}\left(\frac{\sigma}{\delta(x)}\right) \tag{9}$$

The membrane displacement W is then associated with a so-called membrane moment

$$M = D\frac{d^2W}{dx^2}$$

$$= D\left[\alpha R_0 \frac{d^2T}{dx^2} - \frac{\mu R_0}{E}\frac{d^2}{dx^2}\left(\frac{\sigma}{\delta(x)}\right)\right] \tag{10}$$

where

$$D = \frac{E\delta^3}{12(1-\mu^2)} \tag{11}$$

is the generally variable shell rigidity.

2.3 Thermal stresses and displacements in a constant wall thickness circular cylindrical shell with longitudinal temperature variation

Applying the same considerations used in the previous section, we conclude that the stresses are in the axial direction only. However, in the present case of the shell parts I or V (see Figure 1), since the wall thickness is uniform throughout the whole portion, the stress under consideration is constant. We know immediately from equation (1) that

$$\frac{\partial \sigma}{\partial x}\, dx\, \delta = 0 \tag{12}$$

which has the solution

$$\sigma = q_3 \tag{13}$$

where q_3 is another constant of integration.

The stress strain relation may again be written (c.f.2.2)

$$\varepsilon_{xx} = \frac{\partial u}{\partial x} = \frac{1}{E\delta}\sigma + \alpha T \tag{14}_a$$

$$\varepsilon_{ss} = \frac{w}{R_o} = -\frac{\mu}{E\delta}\sigma + \alpha T \tag{14}_b$$

$$\varepsilon_{xs} = \frac{\partial u}{\partial s} = 0 \tag{14}_c$$

$(14)_a$ becomes

$$u(x) = \frac{\sigma}{E\delta}x + \alpha \int_o^x T\, dx + q_4 \tag{15}$$

It is clear, from equation $(14)_c$, that q_4 will not be a function of λ. By substituting (13)

$$u(x) = \frac{q_3}{E\delta}\, x + \alpha \int_0^x T\, dx + q_4 \tag{16}$$

the displacement in the Z direction may be obtained

$$w = -\frac{\mu R_0}{E\delta}\, q_3 + \alpha T R_0 \tag{17}$$

The slope along the axial direction and the bending moment generated from the membrane displacement w are given by the equations (8) and (10).

2.4 Thermal stresses and displacements in a cylindrical shell with corrugated skin subjected to longitudinal temperature variation

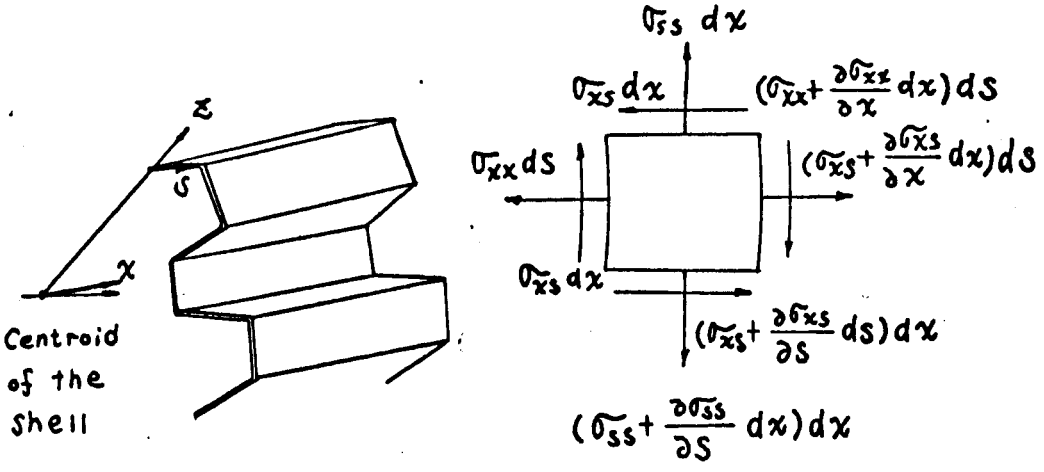

Fig. 3.--Coordinate system for the corrugated skin and the general element

In the cylindrical shell, the equilibrium equations for any arbitrary cross-sectional shape while subjected to no external loading other than heat input may be written

$$\frac{\partial \sigma_{xx}}{\partial x} + \frac{\partial \sigma_{xs}}{\partial s} = 0 \tag{18}$$

$$\frac{\partial \sigma_{ss}}{\partial s} + \frac{\partial \sigma_{xs}}{\partial x} = 0 \tag{19}$$

$$\sigma_{ss} = 0 \tag{20}$$

It should be noted that $\sigma_{xs} = \sigma_{sx}$ indicating moment equilibrium is already taken into account.

The equations give us the arbitrary solutions immediately.

$$\sigma_{xs} = f_1 \tag{21}$$

$$\sigma_{xx} = -\frac{\partial f_1}{\partial s} x + f_2 \tag{22}$$

where f_1 and f_2 will not be function of x, but may be function of s. Equations (21), (22) meet with the requirement that there is no net moment about any diametral axis[4]. Furthermore, since the shell part VII (see Figure 1) is symmetric with respect to the longitudinal axis of the shell, no net shear may be transmitted across a transversal cross-section. Thus

$$\oint_s \sigma_{xx} R_o \cos\phi \, ds = 0 \tag{23}$$

$$\oint_S \sigma_{\tilde{x}x} R_0 \sin\phi \, dS = 0 \tag{24}$$

$$\oint_S \sigma_{\tilde{x}s} R_0 \, dS = 0 \tag{25}$$

$$\oint_S \sigma_{\tilde{x}s} \, dS = 0 \tag{26}$$

where R_0, the radius of curvature of the meridian, is a function of s.

However, in our case the integral of $\sigma_{\tilde{x}x}$ over the cross-section will be constant; and since there is no variation in thickness of the shell, equation (22) must have

$$\frac{\partial f_1}{\partial S} = 0 \tag{27}$$

Hence it is clear f_1 will not be a function of x or s, and (22) may then be written as

$$\sigma_{\tilde{x}x} = f_2 \tag{28}$$

while substituting (21) into (26), and in accompaniment with (27), we have

$$f_1 \oint_S dS = 0 \tag{29}$$

Because of $\oint_S dS \neq 0$ it follows

$$f_1 = 0 \tag{30}$$

and

$$\sigma_{\tilde{x}s} = 0 \tag{31}$$

For convenience we will then denote $\sigma_{\tilde{x}x}$ by σ. The following condition will be true by making use of (28)

$$\oint_S \sigma \, dS = g_5 \tag{32}$$

For consistency with the previous notations, letter g has been used rather than f. g_5 is a function of temperature only, which may be determined by the boundary conditions.

Still, the quantity σ may have variation along δ in viewing the equations (18) and (28).

However, one should realize that the particular coordinate system chosen in the present case ensure us that the displacement along δ will be zero, since the uniform expansion may only take place along the direction of R_0. Besides, knowing that while in the boundary, axial displacement u will not be a function of δ, we then have the following relations

$$\frac{\partial u}{\partial x} = \frac{1}{E\delta}\sigma + \alpha T \tag{33}$$

$$\frac{w}{R_0} = -\frac{\mu}{E\delta}\sigma + \alpha T \tag{34}$$

or

$$u(x) = \frac{\sigma}{E\delta}x + \alpha \int_0^x T \, dx + g_6 \ , \tag{35}$$

where g_6 is a constant and

$$w = -\frac{\mu R_0}{E\delta}\sigma + \alpha R_0 T \tag{36}$$

But the condition for $\frac{\partial u}{\partial S}$ to be zero everywhere enables us to

write

$$\frac{\partial \sigma}{\partial s} = 0 \tag{37}$$

For uniformity, we put

$$\sigma = f_2 = q_7 \tag{38}$$

Equations (35) and (36) may be rewritten as

$$u(x) = \frac{q_7}{E\delta} x + \alpha \int_0^x T\, dx + q_6 \tag{39}$$

$$w = -\frac{\mu R_0}{E\delta} q_7 + \alpha T R_0 \tag{40}$$

Again, the rotation of the tangent of the meridian and the membrane moment generated from the membrane displacement w may be obtained by using the same expressions as (8) and (10).

2.5 Displacements of an elliptical head under uniform temperature distribution

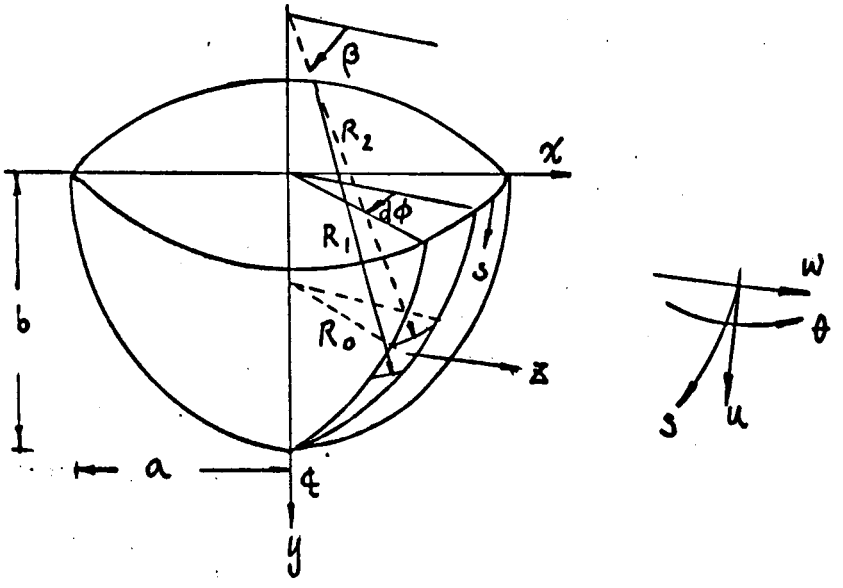

Fig. 4.--Coordinate system of the elliptical head and the convention of signs

The following equations have been derived according to membrane theory and assumption of small displacement by neglecting some of the higher order terms [5]

$$\varepsilon_1 = \frac{1}{R_1}\left[\frac{du}{d\beta} + w\right] \tag{41}$$

$$\varepsilon_2 = \frac{1}{R_0}\left[-u \sin\beta + w \cos\beta\right] \tag{42}$$

and the stress-strain relations

$$\varepsilon_1 = \frac{1}{E}(\sigma_1 - \mu\sigma_2) + \alpha T \tag{43}$$

$$\varepsilon_2 = \frac{1}{E}(\sigma_2 - \mu\sigma_1) + \alpha T \tag{44}$$

We shall consider that the edges of the shell are free from restraints (i.e., $\sigma_1 = \sigma_2 = 0$), hence the above equations take the form

$$\frac{1}{R_1}\left[\frac{du}{d\beta} + w\right] = \alpha T \tag{45}$$

$$\frac{1}{R_0}\left[-u \sin\beta + w \cos\beta\right] = \alpha T \tag{46}$$

On eliminating w from the above two equations, one obtains

$$\frac{du}{d\beta} + u \tan\beta = \alpha T (R_1 - R_2) \tag{47}$$

the general solution of which becomes

$$u = \alpha T \cos\beta \left[\int \frac{R_1 - R_2}{\cos\beta}\, d\beta + C\right] \tag{48}$$

where C is a constant of integration.

By using the following notations

$$K = \frac{a}{b} > 1$$

$$V = \left[K^2 - (K^2-1)\sin^2\beta\right]^{-\frac{1}{2}} = \left[1 + (K^2-1)\cos^2\beta\right]^{-\frac{1}{2}}$$

$$R_1 = K a V^3$$

$$R_2 = K a V \tag{49}$$

$$y = \sqrt{1 - \frac{R_2^2 \cos^2\beta}{a^2}}\, b - b \sin\beta \cdot V$$

equation (48) becomes

$$U = \alpha T \cos\beta \left[K a \int \frac{V^3 - V}{\cos\beta}\, d\beta + C\right] \tag{50}$$

Again, this may be simplified

$$U = -\alpha T \cos\beta \left[K a (K^2-1) V \sin\beta - C\right] \tag{51}$$

(51) can be evaluated exactly

$$U = -\alpha T \cos\beta \left[b (K^2-1) V \sin\beta - C\right] \tag{52}$$

Since we shall deal later with a displacement component Δ which is perpendicular to the axis of revolution, viz.

$$\Delta = -U \sin\beta + W \cos\beta \tag{53}$$

C will be dropped out automatically, so we may write

$$U = -\alpha T R_2 + U \tan\beta \tag{54}$$

Eliminating $\frac{du}{d\beta}$ from equations (45), (47) yields

$$w = \alpha T R_2 + u \operatorname{Tan}\beta \tag{55}$$

and by substituting (54)

$$w = \alpha T \left[R_2 - b(K^2-1)\sigma \sin^2\beta \right] \tag{56}$$

The angular deflection of the tangent to the middle surface of the shell can be written as

$$\theta = \frac{u}{R_1} - \frac{1}{R_1}\frac{dw}{d\beta} \tag{57}$$

by substituting (54) and (56) one obtains

$$\theta = 0 \tag{58}$$

This is true as long as T is constant which was assumed for the elliptical head.

2.6 Solution for the boundary condition

Since there is no constraint to the free expansion or contraction of the tank, the mean value of the thermal stresses across the cross-section must vanish. From equations (3), (13), and (38), we have

$$\sigma = g_1 = g_3 = g_7 = 0 \tag{59}$$

Furthermore, since the longitudinal displacement must be continuous across each of the joints, equations (6), (15), and (35) lead to

$$g_2 = 0 \tag{60}$$

$$g_4 = \alpha \int_0^{l^{II}} T^{II}\, dx \tag{61}$$

$$g_6 = \alpha \int_0^{l^{V}} T^{V}\, dx + \alpha \int_{\cdot}^{l^{II}} T^{II}\, dx \tag{62}$$

where l^{II}, l^{V} denote the length of part II and V respectively. T^{II},

T^{∇} state the temperature distribution of these two parts.

However, we are not interested in the displacement u which is defined by the constants g_2, g_4, and g_6.

By using equations (5), (17), and (36), the radial displacement in the cylindrical shell for all the different sections becomes

$$w = -\alpha R_o T \tag{63}$$

And the rotation in the axial direction will be

$$\theta = -\alpha R_o \frac{dT}{dx} \tag{64}$$

The displacement Δ (c.f.p. 14) and rotation θ at the joint for the semi-elliptical bulkhead are obviously not the same as those from the cylindrical shell by comparing equation (53) with (63), and (58) with (64).

The difference of these may be interpreted by the edge effects of the individual shell parts as developed in the next chapter.

CHAPTER III

EDGE EFFECTS

3.1 Introduction

Due to (a) the abrupt change of wall thickness, (b) the discontinuity of the curvature of the meridian, and (c) the discontinuous gradient of the thermal loading, in certain regions, where continuity of the structure cannot be maintained by membrane forces alone, forces and moments will be induced whose influence is of local character. These edge loadings, as they are usually called, are induced in order to make the rotations and displacements of adjacent walls continuous.

With the continuity of the structure in mind, one may determine the unknown redundance by imagining the shell to be physically separated at the discontinuities. The edges at each cut, in general, will have different amounts of displacements and rotations. A gap is said to be existed, if the membrane stresses alone are considered. To restore the continuity, suitable edge moments and edge shears have to be induced, and the gaps at each discontinuity will vanish.

Having expression for the rotation and displacement at each edge of the discontinuity caused by unit edge shear and moment, it is possible to calculate the edge displacements and rotations of the various shells in terms of the unknown edge loadings. The geometrical compatibility requires the displacements and rotations at the edges of adjacent members to be in equality. A set of simultaneous linear algebraic equations for the redundance yields the solution for the unknowns.

In the first part of the next section, Figure 5 shows the complete unknown redundance, the relative members, and the gaps induced imaginarily. Given in accompany are the compatibility equations which lead to a general formulation.

Generally, for n compatibility equations, a system of linear simultaneous algebraic equations involving n unknown redundance is obtained[6]. However, instead of solving these n simultaneous equations, a step by step procedure has been worked out in the present analysis. The advantage in doing so will be examined later.

Furthermore, consider the abrupt change of wall thickness, the existence of the membrane moment

$$M = D \frac{d^2 W}{d x^2} \tag{65}$$

may have a discontinuity at the joint while membrane stresses alone are considered, thus violating the moment equilibrium across the cut at two adjacent shell members. To restore the continuity, a moment distribution method which induces the suitable edge loadings at the joint has been introduced corresponding to the step by step procedure.

Once the unknown edge loadings have been evaluated, the stresses at each interior point of all the members may be readily obtained by using stress diagrams plotted for individual cases and the displacements and rotations may likewise be computed from the corresponding equations.

3.2 Analytic formulation

Consider the shell shown as Figure 1. We may use the hypothesis touched in the preceding section, that is wherever a change in thickness, curvature or temperature gradient, the shell is imagined to be physically

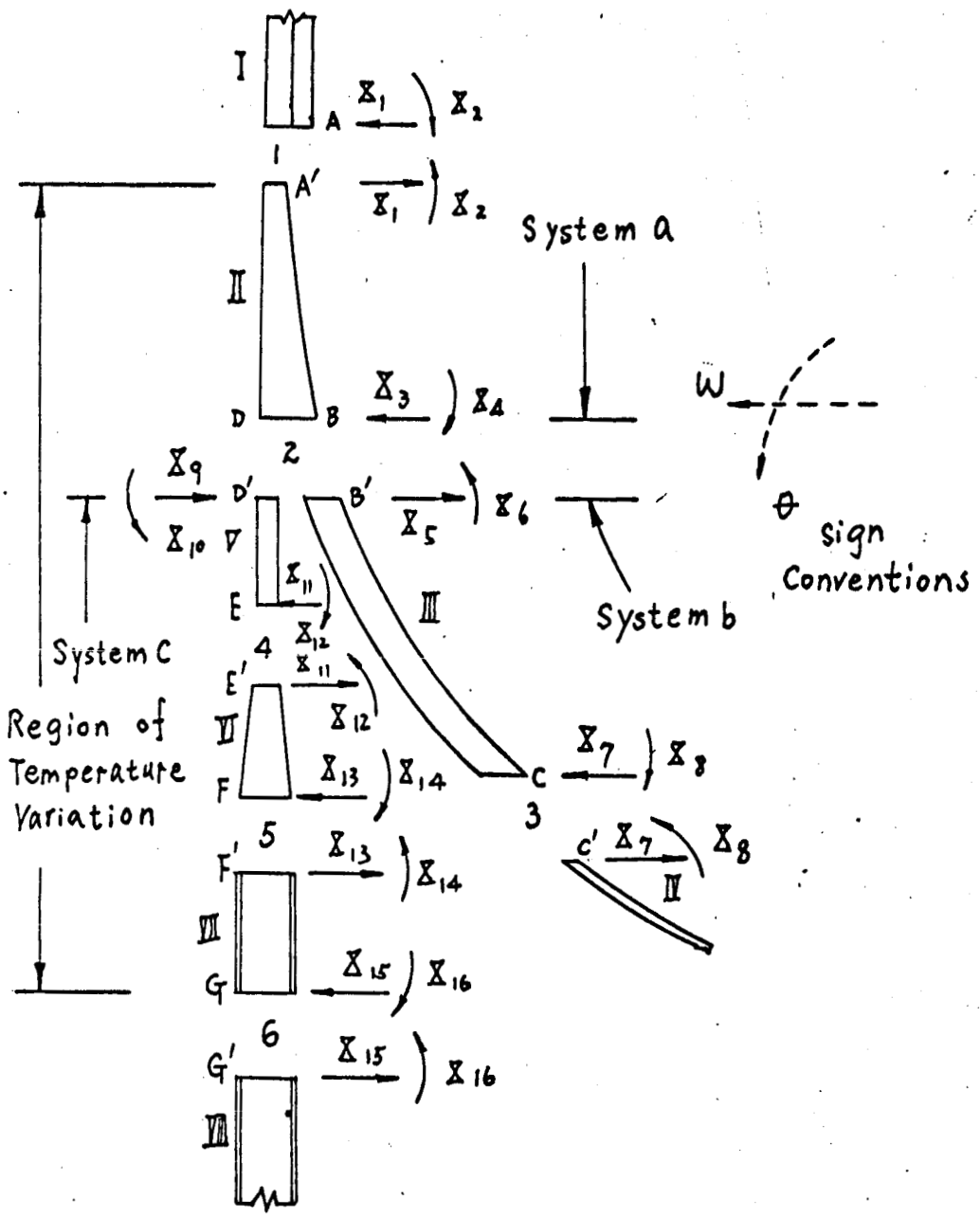

Fig. 5.--Unknown edge moments and edge shears

separated. Considering the membrane stresses alone, the adjacent edges in each cut will have different amounts of displacements and rotations. The gaps occured in edge displacements and rotations require the introducing of edge loadings. To preserve the continuity of the structure, the edge moments and edge shears introduced should be suitable not only for closing the gaps but must also be in self-equilibrium at each cut.

We adopt the following notations by referring to Figure 5.

α_{ij} = The deflection α_i (i.e., displacement w if i is odd and rotation θ if i is even) due to a unit edge load $X_j = 1$. The deformation takes place at that side of a cut which is indicated by an unprimed capital letter (i.e., the letter "A" if $i = 1, 2$; the letter "B" if $i = 3, 4$; the letter "C" if $i = 5,6$; . . . the letter "G" if $i = 11, 12$. One may realize that "B" and "D" are consistent with each other, since they indicate same edge but different cuts of part II).

X_j = Unknown edge load. This is a shear force if j is odd and an edge moment if j is even.

α'_{ij} = The deflection α'_i due to a unit edge loading which takes place at that side of a cut indicated by a primed capital letter. The meaning of i and j is the same as before.

α_{io} = The similar quantity to α_{ij} but due to the thermal loading (membrane stresses).

α'_{io} = The similar quantity to α'_{ij} but due to the thermal loading.

$\delta_{ij} = \alpha_{ij} - \alpha'_{ij}$ — These quantities are called "influence coefficients." They give the relative deformation across the adjacent edges of a cut due to unit edge loadings.

$\delta_{i0} = \alpha_{i0} - \alpha'_{i0}$ = These quantities give the relative deformation across the adjacent edges of a cut due to membrane stresses.

For each cut, the geometrical compatibility requires that the displacement and rotation be continuous at the joint. Figure 5 leads to

$$
\begin{aligned}
&E W_{1A} - E W_{1A'} && E\theta_{1A} - E\theta_{1A'}\\
&E W_{2B} = E W_{2B'} && E\theta_{2B} - E\theta_{2B'}\\
&E W_{2B} - E W_{2D} = E W_{2D'} && E\theta_{2B} = E\theta_{2D} = E\theta_{2D'}\\
&E W_{3C} - E W_{3C'} && E\theta_{3C} = E\theta_{3C'}\\
&E W_{4E} = E W_{4E'} && E\theta_{4E} = E\theta_{4E'}\\
&E W_{5F} = E W_{5F'} && E\theta_{5F} - E\theta_{5F'}\\
&E W_{6G} = E W_{6G'} && E\theta_{6G} = E\theta_{6G'}
\end{aligned}
\qquad (66)
$$

where the subscripts are denoting the cuts and edges at which the deformations take place respectively.

Generally, these 14 compatibility equations together with the following two conditions at the joint DB-D'B' may be solved for the 16 unknowns.

$$
\begin{aligned}
&X_5 R_0^{B'} + X_9 R_0^{D'} = X_3 R_0^{B}\\
&X_6 R_0^{B'} + X_{10} R_0^{D'} = X_4 R_0^{B}
\end{aligned}
\qquad (67)_a
$$

where $R_o^{B'}$, $R_o^{D'}$, R_o^{B} are the radius of curvature of the middle surface of meridian at the cross sections B, D', B respectively. Knowing that $R_o^{B'} : R_o^{B} \approx 1$, $R_o^{D'} : R_o^{B} \approx 1$, we may write

$$\begin{aligned} X_5 + X_9 &= X_3 \\ X_6 + X_{10} &= X_4 \end{aligned} \qquad (67)_b$$

The expressions for the compatibility equations are easily obtained by the use of the edge coefficients α_{ij}, α_{ij}', α_{i0}, α_{i0}', and the edge loadings X_j, as explained previously.

For a simple example, one may take for gap 1, or cut A-A'. According to the linearity of shell theory, the displacement w may be written

$$w_{1A} = \alpha_{11} X_1 + \alpha_{12} X_2 + \alpha_{10} \qquad (68)$$

The cylindrical part I itself is assumed to be long enough so that the cut A may be investigated independently of any other cut, if any, which then has no reaction on A.

Similarly

$$w_{1A}' = \alpha_{11}' X_1 + \alpha_{12}' X_2 + \alpha_{13}' X_3 + \alpha_{14}' X_4 + \alpha_{10}' \qquad (69)$$

where now the terms containing X_3, X_4 describe the reactions from the lower edge.

It is necessary that

$$w_{1A} - w_{1A}' = 0 \qquad (70)$$

for the continuity of the displacements.

Equation (70) may be written

$$\begin{aligned} &(\alpha_{11} - \alpha_{11}') X_1 + (\alpha_{12} - \alpha_{12}') X_2 + (\alpha_{13} - \alpha_{13}') X_3 \\ &+ (\alpha_{14} - \alpha_{14}') X_4 + (\alpha_{10} - \alpha_{10}') = 0 \end{aligned} \qquad (71)$$

In the notation of influence coefficients (c.f.p. 21), it becomes

$$\delta_{11} X_1 + \delta_{12} X_2 + \delta_{13} X_3 + \delta_{14} X_4 + \delta_{10} = 0 \qquad (72)$$

It is clear that equation (72) is the result of the first compatibility equation in (66).

The compatibility equations will in general lead to n simultaneous equations for n unknown redundances, if equation (67) is implicitly involved.

By substituting with equation (67), equation (72) and the subsequent equations may be written in the form

$$\sum_j \delta_{ij} X_j + \delta_{10} = 0 \qquad (73)$$

In matrix form, this becomes

$$\Delta \mathbf{X} + \Delta_0 = 0 \qquad (74)$$

where Δ is a $n \times n$ matrix, the vector $\mathbf{X}$ denotes the n unknown redundances and Δ_0 is a column matrix containing the thermal load.

(74) has the solution

$$\mathbf{X} = -\Delta^{-1} \Delta_0 \qquad (75)$$

If C_i is the circumference of the shell at i, and similarly C_j the circumference at j, Betti's [7] work theorem leads to

$$C_i \delta_{ij} = C_j \delta_{ji} \qquad (76)$$

In case for

$$C_i = C_j \qquad (77)$$

which is, for example, fulfilled by all cylindrical members we have

$$\delta_{ij} = \delta_{ji} \qquad (78)$$

and that is known as Maxwell's reciprocal displacement theorem. Equation

(78) states that the matrix Δ is symmetric in that case.

However, in spite of the above formulation, the method we are employing here in the present analysis is no longer a straightforward form of the $n \times n$ matrix solution as indicated in equations (73) and (74). The difficulty is in the fact that part VI, as shown in Figure 5, cannot be treated as a beam on elastic foundation as longitudinal strips of the cylindrical wall usually can be, because it is formed by individual pieces of clamps connecting the cylindrical part V and the corrugated skin part VII. The simple beam with variable thickness cannot be considered as shell construction. The applying force or moment per inch of the periphery at one edge is no longer in self-equilibrium as it is in a shell. Equations (73) and (74) fail in this case as one may realize that α'_{11j} and α'_{12j}, which represent the edge coefficients at gap 4; and α_{13j}, α_{14j} which represent the edge coefficients at gap 5 for the part to be taken as a free body, do not exist.

The requirement for the equilibrium of part VI forces us to construct an equivalent step by step procedure for solving the whole problem.

The basic idea is to close each of the three systems a, b, c first. It is then possible to obtain the displacement and rotation at B,B' and D' for a unit shear or moment acting at each of the three edges. The moment and shear arised at the joint of each system will be known in the process for calculating the edge coefficients by taking each system as a continuity piece. With the edge coefficients for system a, b, c at hand, gap 2 may then be closed by using the compatibility equations.

By this procedure, the equilibrium state of part VI may be obtained by considering parts V and VI as one piece whenever the edge

coefficients at F are needed, and by considering parts VI, VII, and VIII to be one continuous piece whenever edge coefficients at E' are needed (c.f.p. 44).

We demonstrate here the general considerations and basic equations involved in this step by step procedure. However, it should be pointed out that no analytical formulation for the edge coefficients will be presented in this section. The complete solution in the numerical form will finally be given in the following chapter.

The procedure may be systematized as follows.

(1) Close the gap at the far ends from the gap 2 for each system.

In detail, the compatibility equations are:

For system a, gap 1

$$E W_{1A} = E W_{1A'}$$
$$E \theta_{1A} = E \theta_{1A'} \qquad (79)$$

For system b, gap 3

$$E W_{3C} = E W_{3C'}$$
$$E \theta_{3C} = E \theta_{3C'} \qquad (80)$$

And for system c, gap 6

$$E W_{6G} = E W_{6G'}$$
$$E \theta_{6G} = E \theta_{6G'} \qquad (81)$$

It should be understood that we are now taking the relative displacements and rotations at the cut we choose as a load term (i.e., δ_{io}). Any edge shears and edge moments appear in the compatibility equations should relate to this load term only. Viewing this, each of the above systematic equations may be written in a 2 x 2 matrix form, since it is clear from the above statement that the edges B, B', D' and F' will be

considered to be free at the present time.

We have for gap 1 the equation

$$\begin{pmatrix} \delta_{11} & \delta_{12} \\ \delta_{21} & \delta_{22} \end{pmatrix} \begin{pmatrix} X_1' \\ X_2' \end{pmatrix} + \begin{pmatrix} \delta_{10} \\ \delta_{20} \end{pmatrix} = 0 \tag{82}$$

Here X_1', X_2' are contributions to the resultant edge effects. The influence coefficients δ_{ij} are the same as described previously and δ_{10}, δ_{20} are the relative displacement and relative rotation, respectively, at gap 1 in considering the membrane stresses alone.

Equation (82) can be solved

$$\begin{pmatrix} X_1' \\ X_2' \end{pmatrix} = -\begin{pmatrix} \delta_{11} & \delta_{12} \\ \delta_{21} & \delta_{22} \end{pmatrix}^{-1} \begin{pmatrix} \delta_{10} \\ \delta_{20} \end{pmatrix} \tag{83}$$

For gap 3 and 6, similar equations as equation (83) may be established.

It should be noted further, that in closing the gaps 1, 3, and 6, some additional contributions to the displacements and rotations at the edges B, B', and F' will be induced. These effects have to be taken into consideration later.

(2) In closing the gaps of system c, one has to consider V and VI as well as VI, VII and VIII as separate continuity pieces. Since VII and VIII are of the same cylinder it is possible to take it as one piece of a semi-infinite beam on elastic foundation. The edge moment and shear then occurring at G and G' from the redundance at edge F' may be obtained from the equations of beams on elastic foundation [3].

In taking V and VI as a continuity piece, it is necessary, according to the present hypothesis, to take edge D' as a free edge while gap 4 and 5 are treated.

The edge deformation coefficients at the edge F for pieces V and VI will be taken care of in the next chapter.

Gap 4, again, may be evaluated by an equation similar to equation (83) by considering VI, VII and VIII as one piece. The effects on gap 5 and 6 from the edge loadings X_1', and X_2' where the prime denotes the fact that the edge quantity X_j' is only part of the final value X_j are readily obtained, once the edge moments and shears at each cut for edge unit loadings at E' have been prepared.

The edge deformation coefficients for any such combined piece may be computed with the same notion as is shown with the following example, where only the shear force X_3 is acting at B.

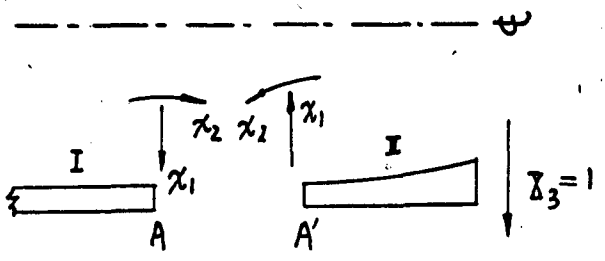

Fig. 6.--Edge coefficients for combined pieces

Small χ_κ means the edge effects from the loading X_3. A similar configuration is valid in case the edge moment X_4 is acting at B. Although Figure 6 shows the gap 1 only, it is true for any other system.

The relative displacement and rotation over the gap 1 will now be displacement and rotation at edge A' from the unit shear $X_3 = 1$.

The geometrical compatibility leads to the result

$$\begin{pmatrix} \chi_1 \\ \chi_2 \end{pmatrix} = - \begin{pmatrix} \delta_{11} & \delta_{12} \\ \delta_{21} & \delta_{22} \end{pmatrix}^{-1} \begin{pmatrix} \delta_{10} \\ \delta_{20} \end{pmatrix} \qquad (84)$$

where δ_{10}, δ_{20} are from the applied unit load $X_3 = 1$ only.

The edge deformation coefficients for the system a become

$$\alpha_{33}^{a} = \alpha_{33} \cdot 1 + \alpha_{31} \cdot \chi_1 + \alpha_{32} \cdot \chi_2 \tag{85}$$

where superscript a means system a as one piece is considered.

Similarly, for a unit moment $X_4 = 1$, the edge deformation coefficients for the system a become

$$\alpha_{44}^{a} = \alpha_{44} \cdot 1 + \alpha_{41} \cdot \chi_1^{*} + \alpha_{42} \chi_2^{*} \tag{86}$$

where χ_1^{*}, χ_2^{*} means the edge effects from the unit moment $X_4 = 1$ at B or D.

With the general formulation, edge effects for any combined system may be evaluated with the help of equations (85) and (86).

(3) With the continuity of each system in mind, we may try to close gap 2, the joint of the three systems. The compatibility equations

$$\begin{aligned} E W_{2B} &= E W_{2B'} & E \theta_{2B} &= E \theta_{2B'} \\ E W_{2B} &= E W_{2D'} & E \theta_{2B} &= E \theta_{2D'} \end{aligned} \tag{87}$$

together with

$$\begin{aligned} X_3' &= X_5' + X_9' \\ X_4' &= X_6' + X_{10}' \end{aligned} \tag{88}$$

which may refer to $(67)_b$. Where a prime is to differ from the final value. Equation (88) leads to a 4 x 4 matrix equation, which may be solved for these unknowns.

However, for the sake of simplicity, we will deal with 2 x 2 matrix equations only.

The continuity between system a and b may be restored first.

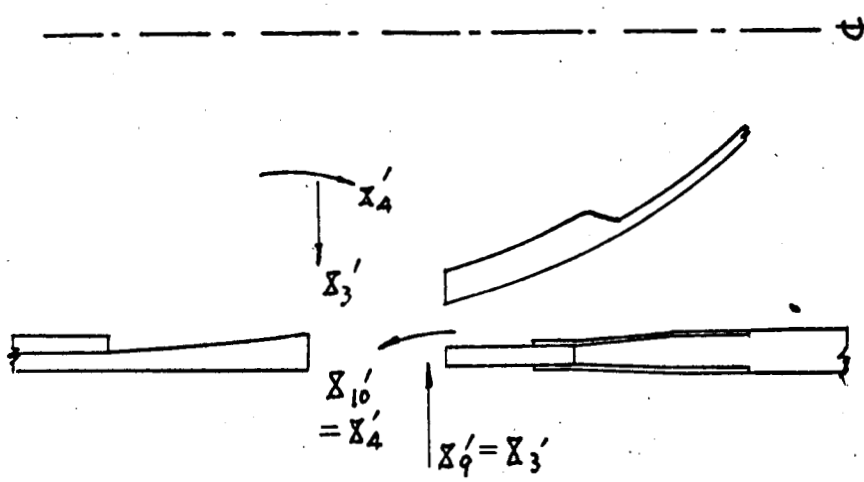

Fig. 7.--Edge effects for the continuity of the displacements on the systems 1 and 2

We have

$$\begin{pmatrix} \delta_{33}^{a,c} & \delta_{34}^{a,c} \\ \delta_{43}^{a,c} & \delta_{44}^{a,c} \end{pmatrix} \begin{pmatrix} X_3' \\ X_4' \end{pmatrix} = - \begin{pmatrix} \delta_{30}^{a,c} \\ \delta_{40}^{a,c} \end{pmatrix} \tag{89}$$

where the superscripts a, c represent the influence coefficients for system a and c.

Again the primed quantities indicate that the unknowns X_j' are only parts of the final values X_j.

One may then obtain the combined deformation for the closed system a and c which we shall denote by ψ and Γ for displacement and rotation, respectively, i.e.,

$$\begin{aligned} \alpha_{30}^{a} + \alpha_{33}^{a} X_3' + \alpha_{34}^{a} X_4' &= \psi \\ \alpha_{40}^{a} + \alpha_{43}^{a} X_3' + \alpha_{44}^{a} X_4' &= \Gamma \end{aligned} \tag{90}$$

where superscript a means system a, and ψ, Γ are the displacement and

rotation for the now continuous pieces system a and system c.

The systems a, b and c may be closed by introducing the edge loading solved from the following equations

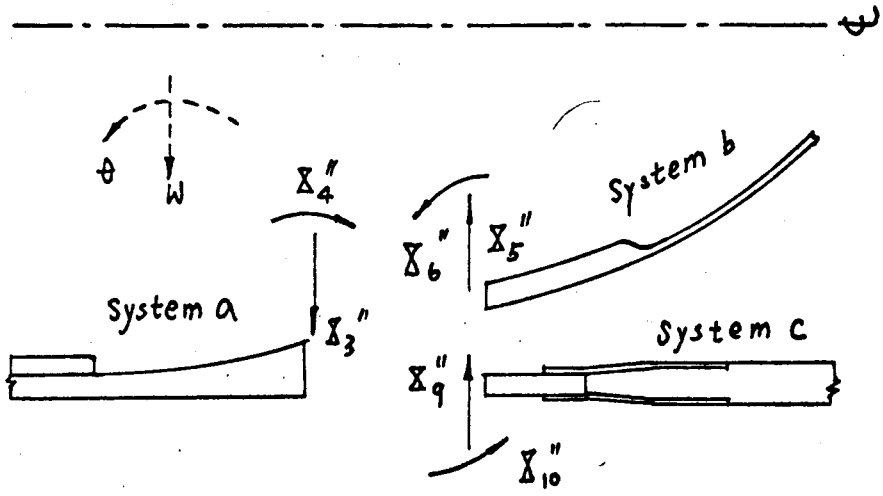

Fig. 8.--Edge effects for the continuity of the displacements on the system of a, b, and c

$$\begin{pmatrix} X_5'' \\ X_6'' \end{pmatrix} = -\begin{pmatrix} \alpha_{35}^b & \alpha_{36}^b \\ \alpha_{45}^b & \alpha_{46}^b \end{pmatrix}^{-1} \begin{pmatrix} \alpha_{30}^b - \psi - \alpha_{39}^c X_9'' - \alpha_{49}^c X_{10}'' \\ \alpha_{40}^b - r - \alpha_{3(10)}^c X_9'' - \alpha_{4(10)} X_{10}'' \end{pmatrix} \quad (91)$$

Where superscripts a, b, and c are for the systems a, b, and c respectively, and double prime indicates the quantities arised are contributions to the unprimed system.

From

$$E W_{2D'} = E W_{2B} \qquad E \theta_{2D'} - E \theta_{2B}$$

$$E W_{2B'} = E W_{2B} \qquad E \theta_{2B'} - E \theta_{2B} \quad (92)$$

we have

$$\begin{pmatrix} X''_9 \\ X''_{10} \end{pmatrix} = \begin{pmatrix} \alpha^c_{39} & \alpha^c_{3(10)} \\ \alpha^c_{49} & \alpha^c_{4(10)} \end{pmatrix}^{-1} \begin{pmatrix} \alpha^a_{33} & \alpha^a_{34} \\ \alpha^a_{43} & \alpha^a_{44} \end{pmatrix} \begin{pmatrix} X''_3 \\ X''_4 \end{pmatrix} \tag{93}$$

and

$$\begin{pmatrix} X''_9 \\ X''_{10} \end{pmatrix} = \begin{pmatrix} \alpha^a_{33}+\alpha^b_{35} & \alpha^a_{34}+\alpha^b_{36} \\ \alpha^a_{43}+\alpha^b_{45} & \alpha^a_{44}+\alpha^b_{46} \end{pmatrix}^{-1} \begin{pmatrix} \alpha^a_{33} & \alpha^a_{34} \\ \alpha^a_{43} & \alpha^a_{44} \end{pmatrix} \begin{pmatrix} X''_5 \\ X''_6 \end{pmatrix} \tag{94}$$

Write

$$\begin{pmatrix} \alpha^a_{33}+\alpha^b_{35} & \alpha^a_{34}+\alpha^b_{36} \\ \alpha^a_{43}+\alpha^b_{45} & \alpha^a_{44}+\alpha^b_{46} \end{pmatrix}^{-1} \begin{pmatrix} \alpha^a_{33} & \alpha^a_{34} \\ \alpha^a_{43} & \alpha^a_{44} \end{pmatrix} = \begin{pmatrix} a_{11} & a_{12} \\ a_{21} & a_{22} \end{pmatrix} \tag{95}$$

By using (95), (92) may be rearranged with the substitution of equation (94).

$$\begin{pmatrix} X''_5 \\ X''_6 \end{pmatrix} = \begin{pmatrix} \alpha^b_{35}+\alpha^c_{39}\cdot a_{11}+\alpha^c_{3(10)}\, a_{21} & \alpha^b_{36}+\alpha^c_{39}\, a_{12}+\alpha^c_{3(10)}\, a_{22} \\ \alpha^b_{45}+\alpha^c_{49}\cdot a_{11}+\alpha^c_{4(10)}\cdot a_{21} & \alpha^b_{46}+\alpha^c_{49}\, a_{12}+\alpha^c_{4(10)}\, a_{22} \end{pmatrix}^{-1} \begin{pmatrix} \alpha^b_{30}-\beta \\ \alpha^b_{40}-1 \end{pmatrix} \tag{96}$$

One has the complete solution for the edge loading of gap 2 by summing up the edge effects arised at each occasion treated previously as

$$\begin{aligned} X_3 &= X'_3 + X''_3 \\ X_4 &= X'_4 + X''_4 \\ X_5 &= X''_5 \\ X_6 &= X''_6 \\ X_9 &= X'_9 + X''_9 \\ X_{10} &= X'_{10} + X''_{10} \end{aligned} \tag{97}$$

3.3 Moment distribution

In considering the membrane stresses alone, the existence of the second derivative of the normal displacement w with respect to x may generate the intrinsic membrane moment

$$M = D \frac{d^2 w}{dx^2} \tag{98}$$

where

$$D = \frac{E \delta^3}{12(1-\mu^2)} \tag{99}$$

and δ thickness of the shell.

Wherever δ has a sudden change over the joint, the intrinsic bending moment M will be a step function at this point. To restore the continuity, the shell may be imagined to be physically separated. One may release the unbalanced moment M at this edge by applying a moment in equilibrium with the unbalanced one. The displacement and rotation caused by this applying moment may form an additional result over the relative displacement and rotation at the gap, and the equation obtained in the previous part may be employed readily to close the gap. The edge moment introduced together with the original unbalanced one and the edge shear induced may form an equilibrium system and continuous over the point that physicially separated.

However, in viewing the process itself brings to a complicate situation when the joint is no longer simply connected, while to release the unbalanced moment means to transfer the problem into the form which may be solved by using equation (96). A moment distribution method is introduced as the following.

Suppose point A has a step function of the intrinsic moment M_0, applying a moment M which is physically balanced with the original

moment.

Introduce now the cut.

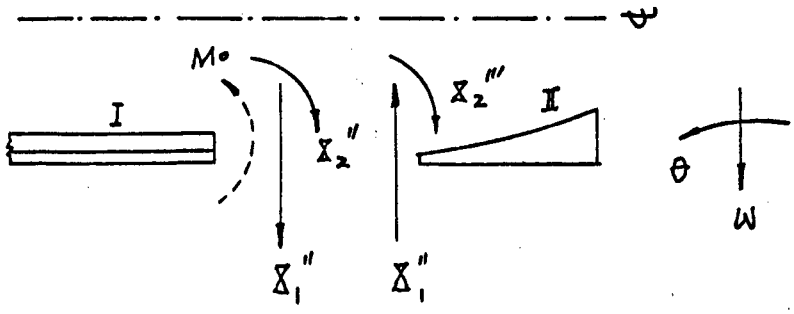

Fig. 9.--Edge effects from the applied moment

where the moment indicated by the dotted line is the intrinsic unbalanced one.

The following conditions must be satisfied.

$$X_2''' + X_2'' = M_0 \tag{100}$$

$$\begin{pmatrix} \delta_{11} & \alpha_{12} & \alpha_{12}' \\ \delta_{21} & \alpha_{22} & \alpha_{22}' \end{pmatrix} \begin{pmatrix} X_1'' \\ X_2'' \\ X_2''' \end{pmatrix} = 0 \tag{101}$$

by substituting (100), equation (101) may be solved

$$\begin{pmatrix} X_1'' \\ X_2''' \end{pmatrix} = \begin{pmatrix} \delta_{11} & \delta_{12} \\ \delta_{21} & \delta_{22} \end{pmatrix}^{-1} \begin{pmatrix} \alpha_{12} \\ \alpha_{22} \end{pmatrix} M_0 \tag{102}$$

Consider the case for gap 2. It is possible to use the same approach by applying a moment M which will be physically equilibrium with the sum of the intrinsic bending moment over edge B, B', and D'.

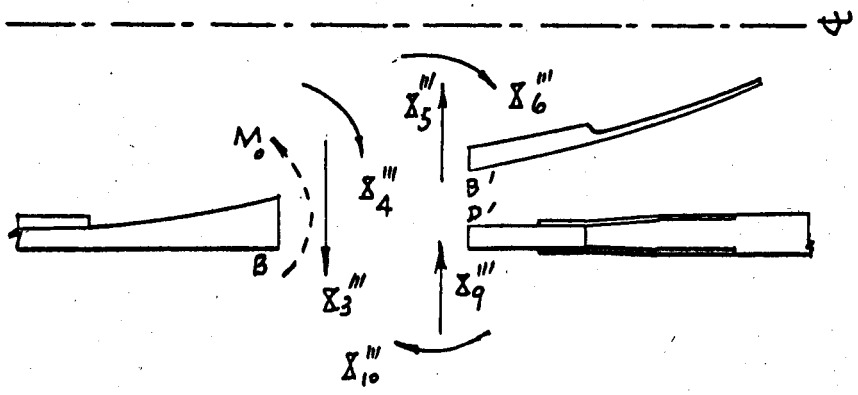

Fig. 10.--Moment distribution for the joint connecting system a, b, c

Again, the moment indicated by the dotted line is the intrinsic unbalanced moments.

It is necessary that

$$\begin{pmatrix} X_3''' \\ X_4''' \end{pmatrix} + \begin{pmatrix} -X_5''' \\ X_6''' \end{pmatrix} + \begin{pmatrix} -X_9''' \\ X_{10}''' \end{pmatrix} = \begin{pmatrix} 0 \\ M_0 \end{pmatrix} \tag{103}$$

Furthermore,

$$E W_{2B} = E W_{2B'} \qquad E\theta_{2B} = E\theta_{2B'}$$

$$E W_{2B} - E W_{2D'} \qquad E\theta_{2B} - E\theta_{2D'} \tag{104}$$

On examining equations(103) and (104), we have

$$\begin{pmatrix} X_3''' \\ X_4''' \end{pmatrix} = -\left\{ \begin{pmatrix} 1 & 0 \\ 0 & 1 \end{pmatrix} + \left[\begin{pmatrix} \alpha_{39}^c & \alpha_{3(10)}^c \\ \alpha_{49}^c & \alpha_{4(10)}^c \end{pmatrix}^{-1} + \begin{pmatrix} \alpha_{35}^b & \alpha_{36}^b \\ \alpha_{45}^b & \alpha_{46}^b \end{pmatrix}^{-1} \right] \begin{pmatrix} \alpha_{33}^a & \alpha_{34}^a \\ \alpha_{43}^a & \alpha_{44}^a \end{pmatrix} \right\}^{-1} \tag{105}$$

The 2 x 2 matrix involved in this process is nevertheless a simple form of calculation. Besides, the solution for each step is not only easily checked, but also the influence for each step to the whole analysis may be seen clearly.

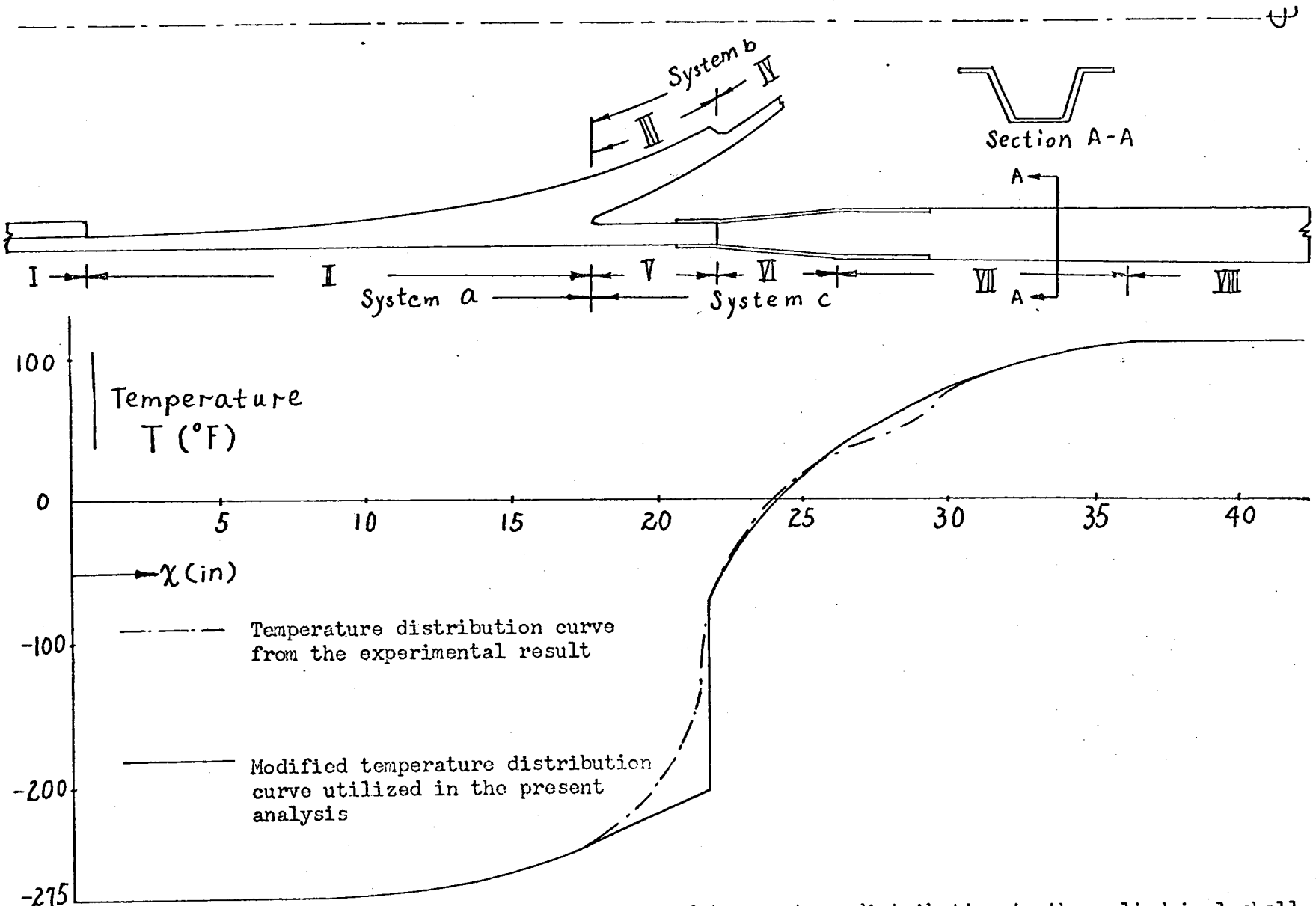

Fig. 11.--Illustrating construction of the joint and temperature distribution in the cylindrical shell

CHAPTER IV

NUMERICAL PROCEDURE

4.1 Description of the construction of the joint

The solution has been carried out with the following geometrical characteristics:

1. The semi-elliptical bulkhead.

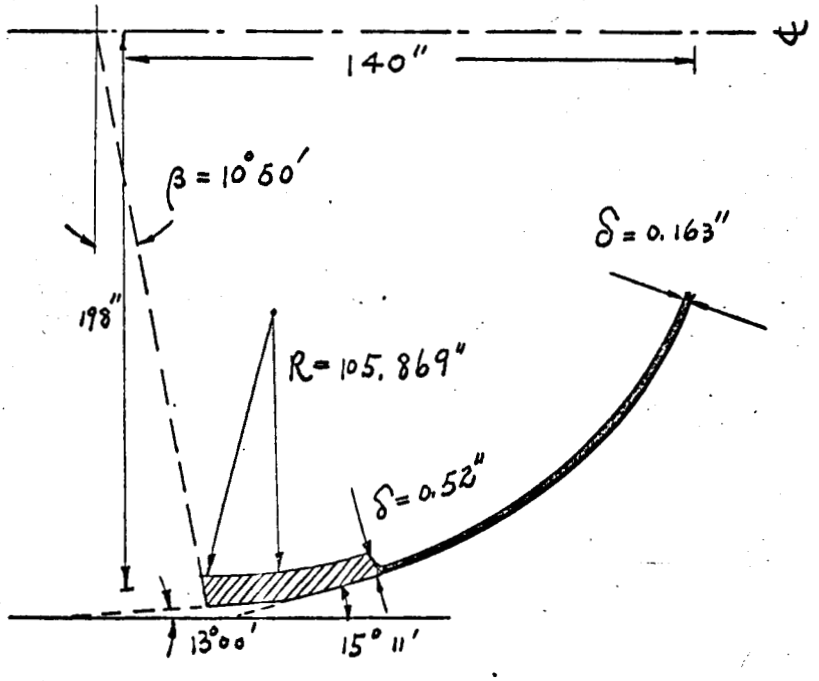

Fig. 12.--Construction of the semi-elliptical bulkhead

2. The cylindrical part of the shell may be divided into several parts, the upper cylindrical shell and the lower intertank skirt. The upper part itself consists of two cylinders one of assumed linear thickness variation from 2.32" to 0.8" and another cylinder reinforced by stif-

fenors with equivalent thickness from the moment of inertia of 1". While the lower portion consists of a plain cylindrical part with a thickness of 1.47" (c.f. 2.3, 2.4). The radius of the cylindrical shell has been taken to be the same as 198" throughout.

3. The boundary condition is assumed to be the same as described in section 2.5.

4. $\alpha = 13 \times 10^{-6}$, $E = 10.6 \times 10^{6}$. Material is aluminum.

5. Temperature distribution is illustrated in Figure 11; the semi-elliptical part has no temperature variation.

6. The reference temperature T_0 is taken to be 100° F.

4.2 Edge deformation coefficients

(1) System a

We consider a general member of this system subjected to edge moments and edge shears at both ends.

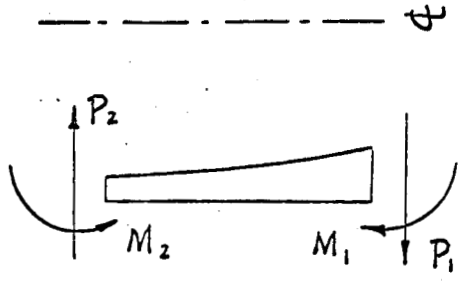

Fig. 13.--General member and sign conventions for the edge moments and edge shears

The sign conventions for the edge coefficients are according to the applied edge loadings and the signs for the displacement and rotation. In the following whenever the edge coefficients at the right of a cut are needed, the coefficients obtained are from the applying edge loadings at the left hand side of Figure 12, according to the sign conventions for the displacement and rotation. And the edge loadings shown in the right

hand side of Figure 12 have the same sign to the edge loadings applied at the left hand edge of any cut.

The edge coefficients in the plain cylindrical part of the upper cylindrical shell (part I) have been treated as semi-infinite beams on elastic foundation which is due to Hetenyi [9].

The coefficients below are for the edge loadings at the right hand edge of part I, and the edge loadings have the same sign as the edge loadings figured at the right hand side of Figure 11.

	P_1	M_1
W_A	0.23800 | -4*	0.21634 | -4
θ_A	-0.21634 | -4	-0.39330 | -5

(106)

the subscripts for deformations indicate the edge shown in Figure 5.

For part II, the cylindrical shell with the assumed linear wall thickness variation, the homogeneous equation of the bending theory reads [8]

$$\frac{d^2}{dx^2}\left(D\frac{d^2w}{dx^2}\right) + \frac{E\delta w}{R_o^2} = 0 \qquad (107)$$

where R_o is the radius of the cylindrical shell, δ the variable thickness of the shell and D the variable shell rigidity. Equation (107) can be solved by means of modified Bessel functions [9].

The solution from digital computer led to the following results (see Figure 13)

	P_1	M_1	P_2	M_2
W_B	0.164 | -3	0.163 | -4	0.104 | -3	-0.145 | -4
θ_B	0.163 | -4	-0.243 | -5	-0.207 | -4	0.190 | -5
W_A,	-0.104 | -3	-0.207 | -4	-0.284 | -3	0.261 | -4
θ_A,	-0.145 | -4	-0.190 | -5	-0.261 | -4	0.440 | -5

(108)

*0.23800 | -4 read 0.23800×10^{-4}

In order to conform this linear assumption of the thickness variation, an analogous method of model test has been accomplished. The result from a Moiré model test which simulated the finite beam on the elastic foundation is as follows [9]

	P_1		M_1		P_2		M_2	
W_B	0.189	-3	0.167	-4	0.101	-3	-0.150	-4
θ_B	-0.167	-4	-0.244	-5	-0.200	-4	0.189	-5
W_A,	-0.101	-3	-0.200	-4	-0.237	-3	0.259	-4
θ_A,	-0.150	-4	-0.189	-5	-0.259	-4	0.439	-5

(109)

On comparing (108) with (109), it can be seen that they are in good agreement. In what follows the values from equation (109) will be utilized.

For the whole upper cylindrical part, the deformation coefficients caused by the edge loadings

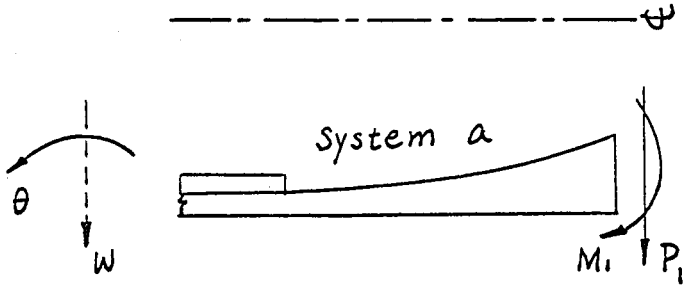

Fig. 14.--Edge loadings on system a

may be obtained by closing the gap in between the joint of part I and part II imposed by the applied unit edge loadings. The quantities computed from the equations (85) and (86) are:

	P_1		M_1	
W_B	0.14300	-3	0.09540	-4
θ_B	-0.09540	-4	-0.12448	-5
W_A	-0.01017	-3	-0.051140	-4

	P_1		M_1	
θ_A	-0.014211	-4	0.00588	-5

(110)

(2) System b

In studying the edge coefficients of the knuckle part, a Geckler-type approximation has been used [9]. The solution of the governing equation

$$\frac{d^2}{dS^2}\left(D\,\frac{d^3 W_n}{dS^3}\right) + \frac{E\delta}{R_m^2}\,\frac{dW_n}{dS} = 0 \tag{111}$$

contains Kelvin functions. Where S is the arc length of the toroidal shell, D the shell rigidity, $\delta = \delta_0(1+aS)$ the assumed linearly variable thickness, E the modulus of elasticity, R_m the averaged radius of curvature, and W_n the normal displacement. By some algebraic transformation of the solution of equation (111), the following edge coefficients for the knuckle have been carried out by an IBM 709 digital computer (see Figure 13).

	P_1		M_1		P_2		M_2	
W_B,	-0.44996	-3	-0.12913	-3	-0.782631	-3	0.14177	-3
θ_B,	-0.14402	-3	-0.26974	-4	-0.14177	-3	0.34484	-4
W_C	0.10265	-2	0.15229	-3	0.44996	-3	-0.14402	-3
θ_C	-0.15229	-3	-0.35991	-4	-0.12913	-3	0.26974	-4

(112)

where W_B, and W_C are all displacements shown as Figure 13.

The edge coefficients obtained by applying unit shear and unit moment at the edge of the elliptical head are due to an approximate method from Novozhilov [10].

We have

$$\Delta = \alpha_{11} P_2 + \alpha_{12} M_2$$

$$\theta = \alpha_{21} P_2 + \alpha_{22} M_2 \tag{113}$$

where Δ is the displacement described by (53)

and

$$\alpha_{11} = \frac{2\sqrt[4]{3(1-\nu^2)}}{E}\left(\frac{R_2}{h}\right)^{3/2}\sin^2\phi_1$$
$$\alpha_{12} = \alpha_{21} = -\frac{\sqrt{12(1-\nu^2)}}{E\,h^2}R_2\sin\phi_1 \qquad (114)$$
$$\alpha_{22} = \frac{4[3(1-\nu^2)]^{3/4}}{Eh^2}\sqrt{\frac{P_2}{h}}$$

with R_2 as the second principal radius of curvature of the middle surface.

The following coefficients are obtained (see Figure 13)

	P_2	M_2
Δ	0.43870 | -2	0.79581 | -3
θ	0.79581 | -3	0.39507 | -3

(115)

For the whole bulkhead, the edge coefficients may be obtained by closing the gap caused from the displacements discontinuity with the applied edge loading.

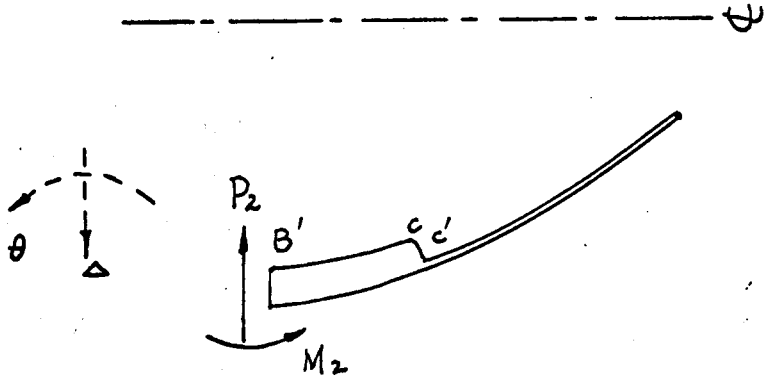

Fig. 15.--Edge loadings on system b

The numerical quantities accomplished by using a desk calculator are as follows.

	P_2	M_2
$W_{B'}$	-0.64845 | -3	0.10643 | -3
$\theta_{B'}$	-0.10643 | -3	0.25009 | -3
W_C	0.21911 | -3	-0.08162 | -3
θ_C	-0.09310 | -3	0.17276 | -4

(116)

(3) System c

The separated parts as V and VII may be considered as finite beams on elastic foundation. The consideration based on Hetenyi [3] gives us (see Figure 13)

for part V

	P_1	M_1
W_E	0.34931 | -2	10.76637 | -4
θ_E	-10.76637 | -4	-4.45286 | -4
$W_{D'}$	-0.17481 | -2	-10.73857 | -4
$\theta_{D'}$	-10.73857 | -4	-4.41834 | -4

(117)

and for part VII

	P_1	M_1
W_G	0.65431 | -3	0.64073 | -4
θ_G	-0.64073 | -4	-0.93448 | -5
$W_{F'}$	-0.31111 | -3	-0.57024 | -4
$\theta_{F'}$	-0.57026 | -4	-0.67161 | -5

(118)

Part VIII has been considered as a semi-infinite beam on elastic foundation. The assumed plain cylindrical shell arrived from a conclusion of section 2.3 leads to the following edge coefficients.

	P_2	M_2
$W_{G'}$	-0.2370|-3	0.01780|-3
$\theta_{G'}$	-0.0178|-3	0.00267|-3

(119)

The quantities described in (119) may as well be used for the system combined with part VII and part VIII.

In order to find the edge coefficients for part VI, it is necessary to take V and VI as well as VI, VII, and VIII to be continuity pieces. Since part VI is not a shell construction but a beam with linearly varying thickness which connects the parts VII and V, the applied unit edge shear or unit edge moment at one end of the clamp cannot establish the equilibrium state alone as it does in the case of a shell.

To take part V and VI as a piece, the edge coefficients at F may be obtained by superposition.

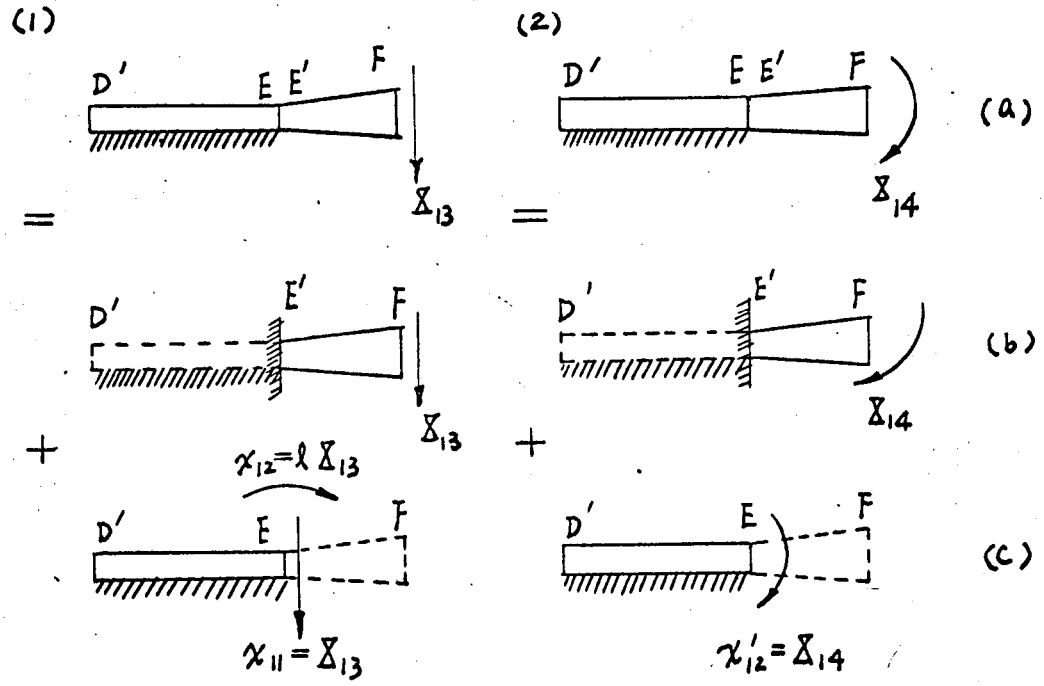

Fig. 16.--Edge loadings for part V and VI

(a) given state of load
(b) + (c) equivalent states to (a)

The displacements and rotations are:

For case (1)

$$\alpha_{9(13)} = \alpha^{VI}_{9(13)} X_{13} + \alpha_{7(11)} \chi_{11} + \left[\alpha_{8(11)} \chi_{11}\right] l + \alpha_{7(12)} \chi_{12} + \left[\alpha_{8(12)} \chi_{12}\right] l \tag{120}$$

and

$$\alpha_{10(13)} = \alpha^{VI}_{10(13)} X_{13} + \alpha_{8(11)} \chi_{11} + \alpha_{8(12)} \chi_{12} \tag{121}$$

For case (2)

$$\alpha_{9(14)} = \alpha^{VI}_{9(14)} X_{14} + \alpha_{7(12)} \chi'_{12} + \left[\alpha_{8(12)} \chi'_{12}\right] l \tag{122}$$

and

$$\alpha_{10(14)} = \alpha^{VI}_{10(14)} X_{14} + \alpha_{8(12)} \chi'_{12} \tag{123}$$

Where notations, except χ_j and χ'_j which denote the edge effects in case (1) and (2), respectively, are the same as used before.

$\alpha^{VI}_{9(13)}$, $\alpha^{VI}_{10(13)}$, $\alpha^{VI}_{9(14)}$, and $\alpha^{VI}_{10(14)}$ are the quantities obtained by considering piece VI as a cantilever beam (p.44).

For $\alpha_{7(11)}$, $\alpha_{7(12)}$, $\alpha_{8(11)}$, $\alpha_{8(12)}$ previous computed numerical values can be used (equation (117)).

One has to realize that the effect of rotation at E will cause an additional displacement at F, which is indicated by

$$(\alpha_{8j} \chi_j) l \tag{124}$$

Taking $X_{13}=1$, and $X_{14}=1$, and in accompanying with the solutions for the cantilever beam (Appendix), we have the following edge coefficients for the combined piece V and VI.

$$\begin{pmatrix} \alpha_{9(13)} & \alpha_{9(14)} \\ \alpha_{10(13)} & \alpha_{10(14)} \end{pmatrix} = \begin{pmatrix} 17.01584|-3, & 2.70399|-3 \\ -2.70399|-3, & -0.45430|-3 \end{pmatrix} \tag{125}$$

it is clear that according to Maxwell's theorem

$$|\alpha_{10(13)}| = |\alpha_{9(14)}| \tag{126}$$

still holds.

For the edge coefficients at E', if one connects part VI with part VII, the same analysis is true. The thickness of the beam, however, will then be

$$h(x) = h_0 + \frac{h-h_0}{l}x \tag{127}$$

instead of the expression formulated in the previous equations (Appendix). h_0 and h are the thickness at E' and F respectively, l is the length of the beam, x the axis with the origin at E' is positive toward the right hand edge F. Equations derived in the Appendix may be used by changing some governing terms.

We have, by taking VII and VIII as a semi-infinite beam on elastic foundation, the edge coefficients for VI, VII, VIII to be a piece are:

$$\begin{pmatrix} \alpha'_{9(13)} & \alpha'_{9(14)} \\ \alpha'_{10(13)} & \alpha'_{10(14)} \end{pmatrix} = \begin{pmatrix} -0.45889|-3 & 0.03557|-3 \\ -0.03557|-3 & 0.01172|-3 \end{pmatrix} \tag{128}$$

Finally, for system c

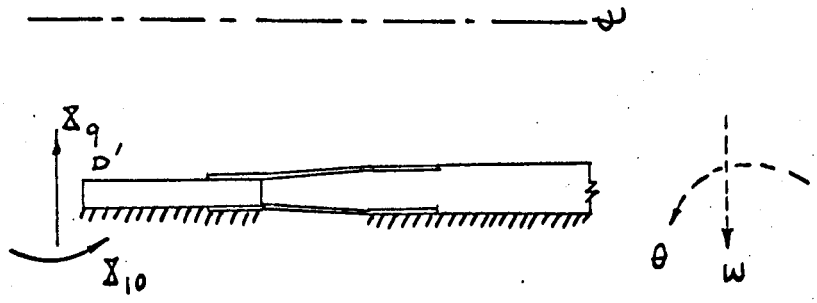

Fig. 17.--Edge loadings on system c

a model of cantilever beams simulating the elastic foundation has been studied. The result is as follows

	X_9	X_{10}
$W_{D'}$	-0.128 | -3	0.029 | -3
$\theta_{D'}$	-0.029 | -3	0.136 | -4

(129)

4.3 Temperature curve and the edge effects

The temperature distribution curve illustrated as in Figure 12 comes from experimental results. The curve plotted shows that in between part V and part VII, due to the construction of the joint, the temperature changes very rapidly. A substitute analytical curve has been adopted in the present analysis as plotted in Figure 12. The modified curve shows good agreement in both the upper cylindrical part and the lower inter-tank skirt. In the joint portion of part V and part VI, a step function has been introduced which represents the sudden change of temperature in the face where the cross sectional area of the shell is a step function itself across the joint.

The temperature curve as shown in Figure 12 has been divided into several sections. It is obvious that different sections introduced by the temperature curve are conform with the choice of the different sections

in the intertank construction itself.

Referring to the coordinate system shown in Figure 11, the temperature equation from the curve fitting may be obtained with a sufficient accuracy as:

For part I and II

$$T = -275\ (^\circ F)\ ,\quad 0 \le x \le 8.5 \tag{130}$$

where x is the axis shown in Figure 11.

Further, still in part II

$$T = -0.00228\,(x-8.5)^4 + 0.06851\,(x-8.5)^3 - 275, \quad 8.5 \le x < 17.5 \tag{131}$$

For part V

$$T = 10(x-17.5) - 240\ ,\quad 17.5 \le x < 21.75$$
$$\Delta T = 71\ (^\circ F) \quad \text{at} \quad x = 21.75 \tag{132}$$

where ΔT represents the jump of the temperature (see Figure 11).

For part VI

$$T = 0.00105\,(x-21.75)^4 - 0.0474\,(x-21.75)^3 + 19.429\,(x-21.75) - 75\ ,\quad 21.75 < x \le 25.35 \tag{133}$$

For part VII

$$T = 0.00105\,(x-21.75)^4 - 0.0474\,(x-21.75)^3 + 19.429\,(x-21.75) - 75\ ,\quad 25.35 < x \le 37.89 \tag{134}$$

It is assumed that the temperature distribution at part VIII is

$$T = 110^\circ\ F \tag{135}$$

throughout, the effect at this portion to the joint of the bulkhead with the cylindrical shell is negligible.

The temperature in the parts III and IV (the bulkhead) is constant throughout and T = -295 (°F).

We shall follow, from now on, the same way as described in Chapter III, to evaluate the problem by considering the continuity of each system from the far end up to the gap 2.

(1) System a

Since the temperature curve shows a constant distribution from χ = 0 to 8.5, there is no discontinuity in between part I and part II as for both the deformation and bending moment from the membrane results are concerned, the system itself is closed except at the gap 2.

By multiplying with $\alpha D R_0$, where D is the bending rigidity, α the thermal expansion coefficient, R_0 the common radius of the cylindrical shell, the second derivative of equation (131) leads to the membrane moment (see equation (10))

$$M = 30964\left[-0.02736(\chi-8.5)^2 - 0.41106(\chi-8.5)\right] \quad (136)$$

$$8.5 \leq \chi \leq 17.5$$

For χ = 17.5, that is at the right edge of part II.

$$M = 45932 \left(\frac{lb\text{-}in}{in}\right) \quad (137)$$

where positive sense means a compressive effect on the outer fiber of the shell.

By using the edge coefficients from equations (110), (116), (129), and the solution of equations (93), (94), and (96), the distribution of the unbalanced moment gives us the following edge loadings.

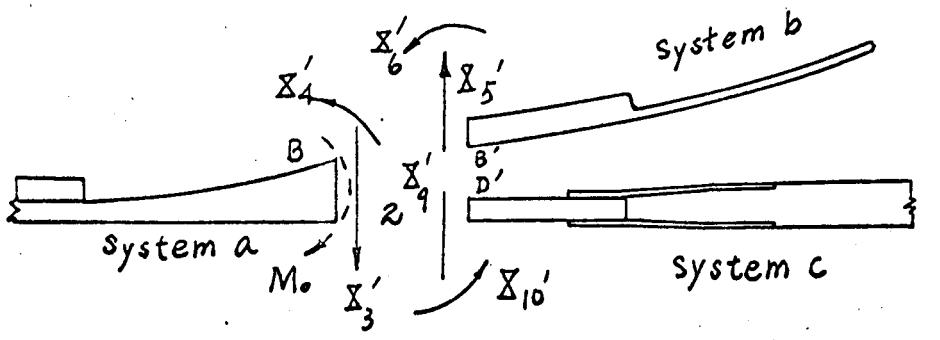

Fig. 18.--Edge loadings at gap 2 from the influence of system a

where moment indicated by dotted line is the intrinsic moment from equation (137).

$$\begin{pmatrix} X_3 \\ X_4 \end{pmatrix} = \begin{pmatrix} 2162 \\ 36936 \end{pmatrix}$$

$$\begin{pmatrix} X_9 \\ X_{10} \end{pmatrix} = \begin{pmatrix} 1414 \\ 4814 \end{pmatrix} \qquad (138)$$

$$\begin{pmatrix} X_5 \\ X_6 \end{pmatrix} = \begin{pmatrix} 748 \\ 4182 \end{pmatrix}$$

where end moment at B is 45932 - 36936 = 8996.

(2) System b

In the semi-elliptical bulkhead, the uniform contraction at the edge B' may be evaluated by using equations (53) and (58)

$$\begin{pmatrix} \alpha^b_{30} \\ \alpha^b_{40} \end{pmatrix} = \begin{pmatrix} -0.51276 \\ 0 \end{pmatrix} \qquad (139)$$

We have the following relative displacement and rotation at B' and D'

$$\begin{pmatrix} \alpha_{30}^{c} - \alpha_{30}^{b} \\ \alpha_{40}^{c} - \alpha_{40}^{b} \end{pmatrix} = \begin{pmatrix} -0.36240 \\ -0.02574 \end{pmatrix} \tag{140}$$

Where χ_{21}' , χ_{22}' in the functions defined γ and Γ in equation (90) are zero, since we take the continuous temperature curve through part V to part VI as a reference.

The solution of equation (96) by referring to Figure 8 gives us:

$$\begin{pmatrix} X_3 \\ X_4 \end{pmatrix} = \begin{pmatrix} 78 \\ 388 \end{pmatrix}$$

$$\begin{pmatrix} X_9 \\ X_{10} \end{pmatrix} = \begin{pmatrix} -264 \\ -653 \end{pmatrix} \tag{141}$$

$$\begin{pmatrix} X_5 \\ X_6 \end{pmatrix} = \begin{pmatrix} 342 \\ 1041 \end{pmatrix}$$

(3) System c

The temperature distribution in the part VII may be rewritten as:

$$T = 0.00105(x-21.75)^4 - 0.0474(x-21.75)^3 + 19.429(x-21.75) - 75$$
$$21.75 \leq x \leq 37.89 \tag{142}$$

The second derivative of equation (142) leads to a moment distribution as:

$$M = 7877\left[0.0126(x-21.75)^2 - 0.284(x-21.75)\right]$$
$$25.35 \leq x \leq 37.89 \tag{143}$$

for $\chi = 37.89$, that is at the right edge of part VII,

$$M_o = -10263 \quad \left(\frac{lb-in}{in}\right) \tag{144}$$

where negative sense means a tensile effect on the outer fiber of the shell.

The distribution of this moment at gap 6, $\chi = 37.89$, gives us

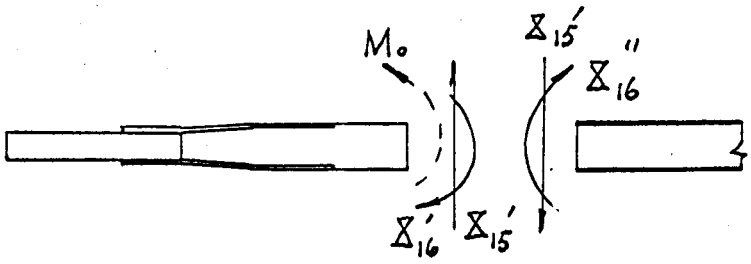

Fig. 19.--Distribution of the unbalanced moment at gap 6

$$\begin{pmatrix} X_{15} \\ X_{16} \end{pmatrix} = \begin{pmatrix} +416 \\ 4442 \end{pmatrix}$$

$$\begin{pmatrix} X_{15} \\ X_{16} \end{pmatrix} = \begin{pmatrix} +416 \\ 5821 \end{pmatrix} \tag{145}$$

Edge loadings X_{15}, X_{16} will have an influence on the displacements at edge D'.

$$\begin{pmatrix} \alpha^c_{30} \\ \alpha^c_{40} \end{pmatrix} = \left(\begin{array}{c|c} -0.41032 & -2 \\ -0.81428 & -2 \end{array}\right) \tag{146}$$

The continuity temperature distribution has the equation across the joint of part VI and VII

$$T = 0.00105(\chi-21.75)^4 - 0.0474(\chi-21.75)^3 + 19.429(\chi-21.75) - 75 \tag{147}$$

second derivative leads to

$$T = 0.0126(\chi - 21.75)^2 - 0.284(\chi - 21.75) \tag{148}$$

by substituting $\chi = 25.35$

$$\frac{\partial^2 T}{\partial \chi^2} = -0.85910 \tag{149}$$

knowing that for the beam

$$M = EI\left(\frac{\partial^2 w}{\partial \chi^2}\right) \tag{150}$$

where EI is the variable bending rigidity of the beam,

and $W = \alpha R_o \frac{\partial^2 T}{\partial \chi^2}$, the displacement of the beam.

Finally, we have the intrinsic membrane moment at F

$$M_F = -5275 \qquad \text{(in-lb/in)} \tag{151}$$

where negative sense states tensile stresses of the outside fiber.

For the edge of F' we have

$$M_{F'} = D\frac{\partial^2 T}{\partial \chi^2}\alpha R_o$$

$$= -6767 \qquad \text{(in-lb/in)} \tag{152}$$

Hence we have for gap 5 the unbalanced moment

$$M_5 = -5275-(-6767) = 1492 \qquad \text{(in-lb/in)} \tag{153}$$

The continuity of the joint may be obtained by applying the moment which equal to the unbalanced one but with different sign. This gives us:

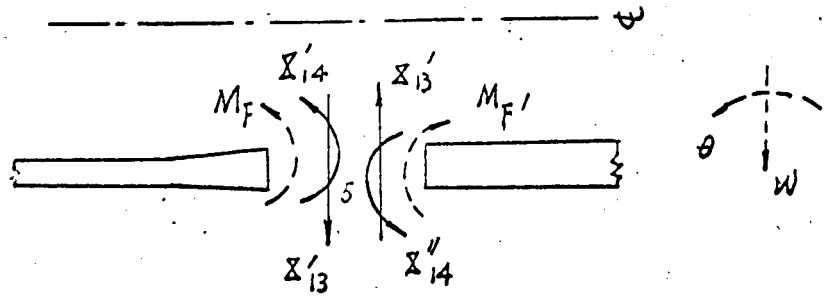

Fig. 20.--Edge effects at gap 5

$$\begin{pmatrix} X_{13} \\ X_{14} \end{pmatrix} = \begin{pmatrix} 34 \\ 210 \end{pmatrix}$$

$$\begin{pmatrix} X_{13} \\ X_{14} \end{pmatrix} = \begin{pmatrix} 34 \\ 1282 \end{pmatrix} \tag{154}$$

where the moments indicated by dotted line are understood to be the intrinsic moments obtained in equations (151) and (152).

The influence of these applied shear and moment at F in order to restore the continuity of gap 5 give us the displacement and rotation at D'.

$$\begin{pmatrix} \alpha^{c}_{30} \\ \alpha^{c}_{40} \end{pmatrix} = \begin{pmatrix} 3.35115 \mid -2 \\ 0.17254 \mid -2 \end{pmatrix} \tag{155}$$

For cut E, E' the relative displacement and rotation obtained from the consideration of the jump of temperature and the slope difference of the right hand edge and the left hand edge temperature curves are:

$$\begin{pmatrix} \alpha'_{70} - \alpha_{70} \\ \alpha'_{80} - \alpha_{80} \end{pmatrix} = \begin{pmatrix} 0.33200 \\ -0.02427 \end{pmatrix} \tag{156}$$

The gap may be closed by introducing the edge moment and edge shear:

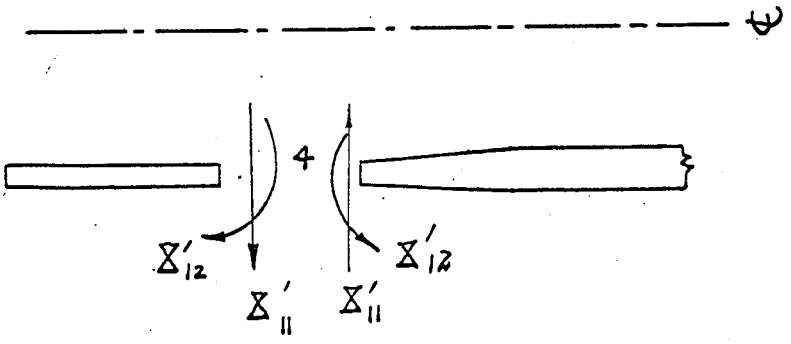

Fig. 21.--Edge loadings at gap 4 from the influence of the step function of the temperature distribution

where

$$\begin{pmatrix} X_{11} \\ X_{12} \end{pmatrix} = \begin{pmatrix} 245 \\ -611 \end{pmatrix} \tag{157}$$

Edge loadings X_{11} and X_{12} will cause additional deformations at edge D' as:

$$\begin{pmatrix} \alpha^{c}_{30} \\ \alpha^{c}_{40} \end{pmatrix} = \begin{pmatrix} 0.22784 \\ 0.00686 \end{pmatrix} \tag{158}$$

The displacements obtained as (146), (155), and (158) at D' give the edge effects at gap 2

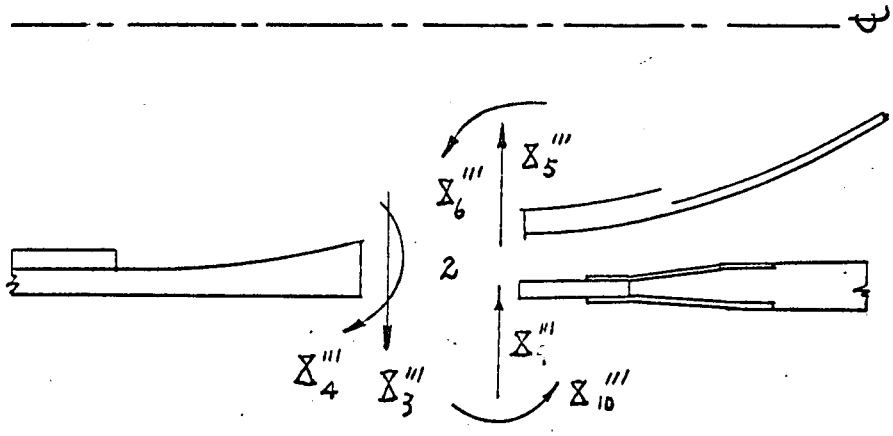

Fig. 22.--Edge loadings at gap 2 from the influence of system c

which has a solution

$$\begin{pmatrix} X_3 \\ X_4 \end{pmatrix} = \begin{pmatrix} 149 \\ 94 \end{pmatrix}$$

$$\begin{pmatrix} X_9 \\ X_{10} \end{pmatrix} = \begin{pmatrix} 243 \\ 563 \end{pmatrix} \tag{159}$$

$$\begin{pmatrix} X_5 \\ X_6 \end{pmatrix} = \begin{pmatrix} -94 \\ -469 \end{pmatrix}.$$

Finally, tho resultant of the edge loadings at the joint of the semi-elliptical bulkhead and the cylindrical shell are as the following by using the same figure as Figure 5.

$$\begin{pmatrix} X_3 \\ X_4 \end{pmatrix} = \begin{pmatrix} 2389 \\ 9478 \end{pmatrix}$$

$$\begin{pmatrix} X_5 \\ X_6 \end{pmatrix} = \begin{pmatrix} 996 \\ 4754 \end{pmatrix} \qquad (160)$$

$$\begin{pmatrix} X_9 \\ X_{10} \end{pmatrix} = \begin{pmatrix} 1393 \\ 4724 \end{pmatrix}$$

Where at B, the intrinsic moment $M_B = 45932$ has been added in X_4.

Few words must be added here, since one may have the question about the quantities of the edge effects in gaps 1, 3, 4, 5, and 6, for restoring the continuity of gap 2, considering each system as a continuity piece. It is easy to see that, in obtaining the edge coefficients at B, B' and D' by considering each system to be continuity piece, the unit edge moment and edge shear applied at each edge of B, B' and D' will arrive the edge effects at each interior joint. Taking these as factors, the final value of the edge effects at each interior joint may then be obtained by multiplying with the resultant edge moment and edge shear as shown in (160) (For X_4, the quantity will be 27363; this is so-called edge effect.), and by summing up the result from closing each of the previous considered gaps.

For a clear view, one may refer to Figures 23, 26, and 29, where the edge effects at each interior joint for the appropriate unit edge moment, edge shear, or distribution moment are obtained for the moment curve. Since membrane stresses $\sigma_x = \sigma_\theta = 0$, the superposition

(c.f.p. 3) leads to the sum of the stresses from the edge loads. The final result in terms of the stresses are plotted according to these moment curves.

We neglect circumferential stresses because (1) membrane $\sigma_\theta = o$

(2) $\sigma_\theta \approx \nu \sigma_x$

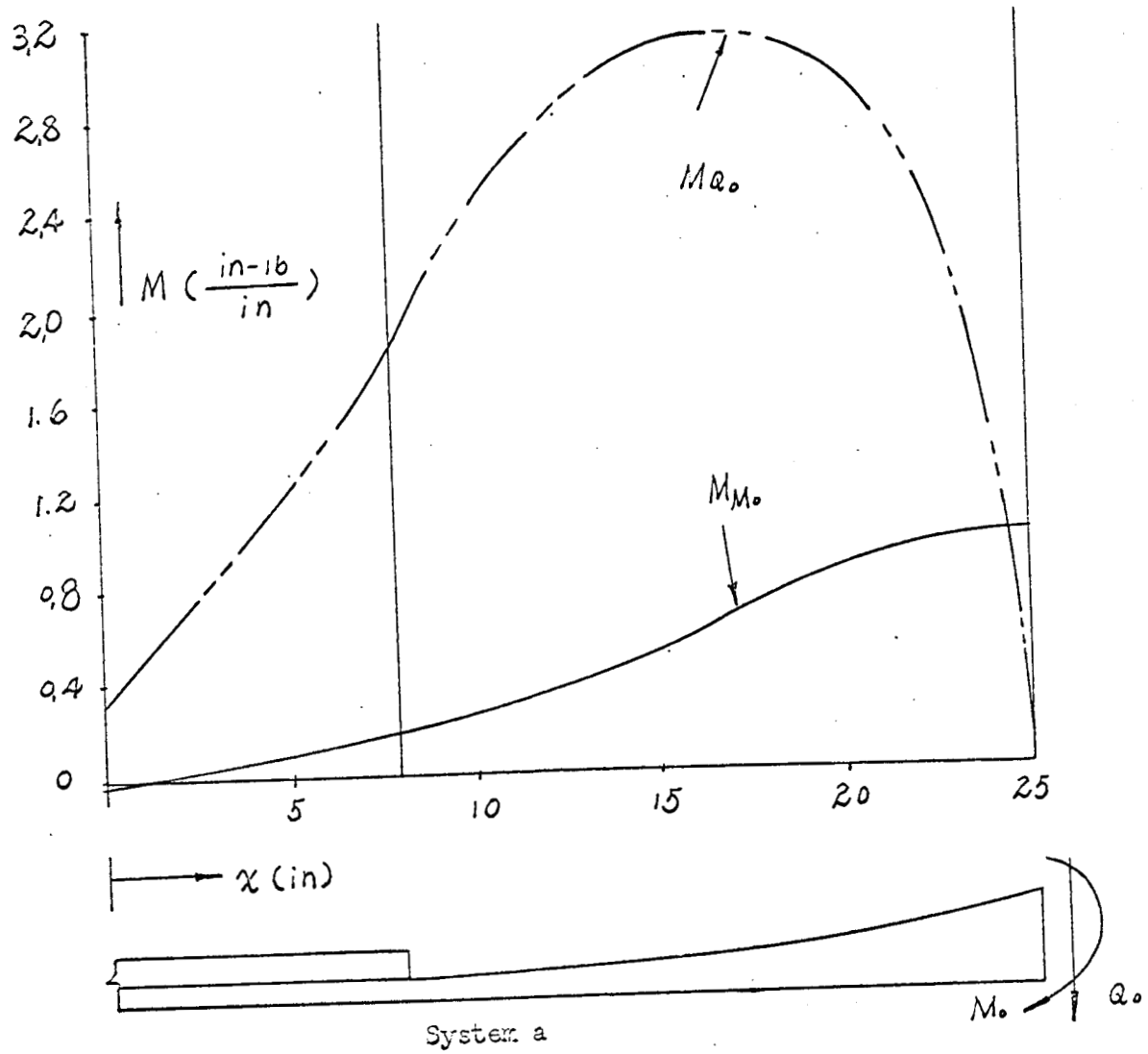

Fig. 23.--Meridional moment distribution in the upper cylindrical part for
$M_o = 1$ and
$Q_o = 1$

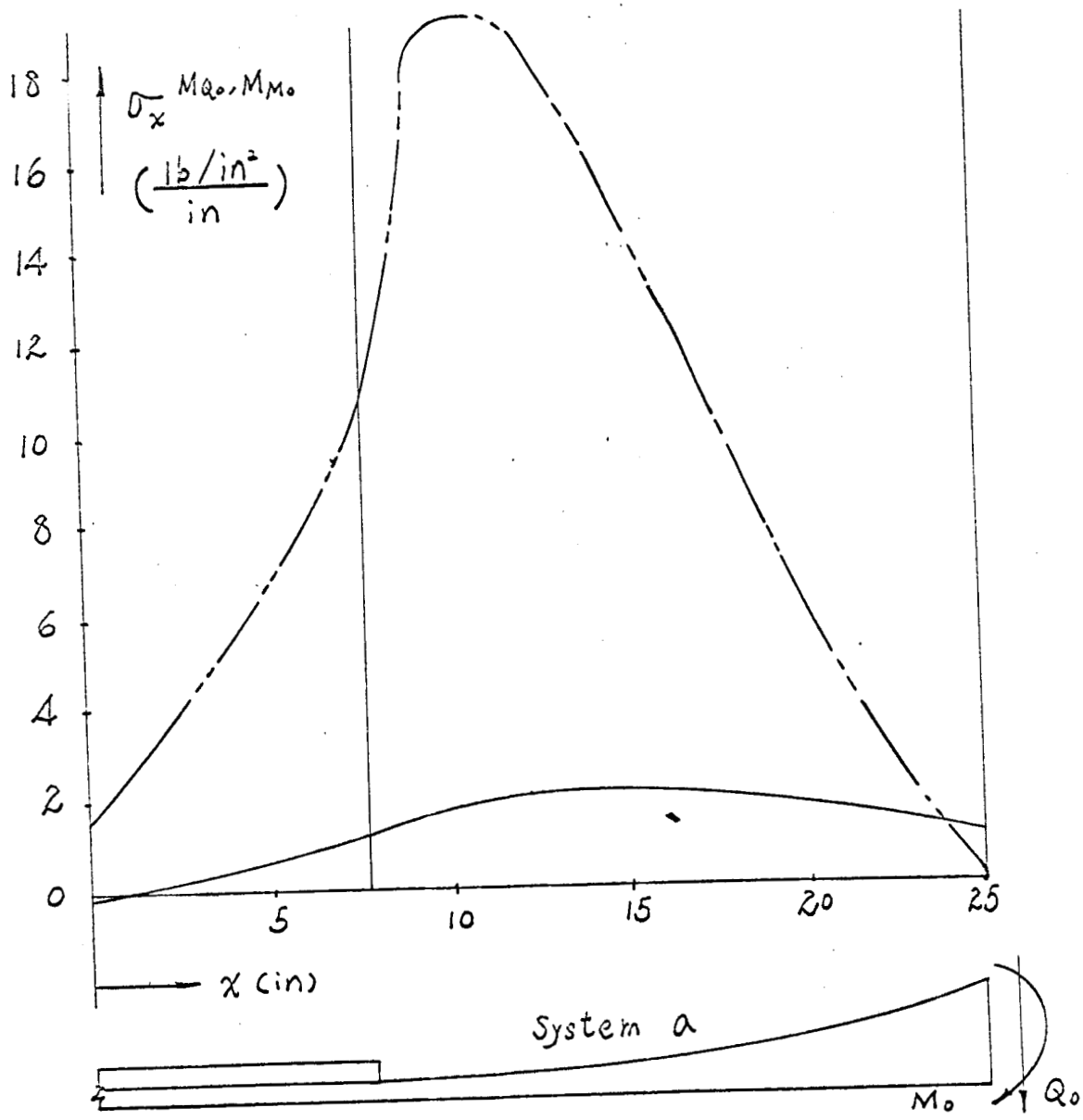

Fig. 24.--Bending stresses in the upper cylindrical part for

$M_0 = 1$
$Q_0 = 1$

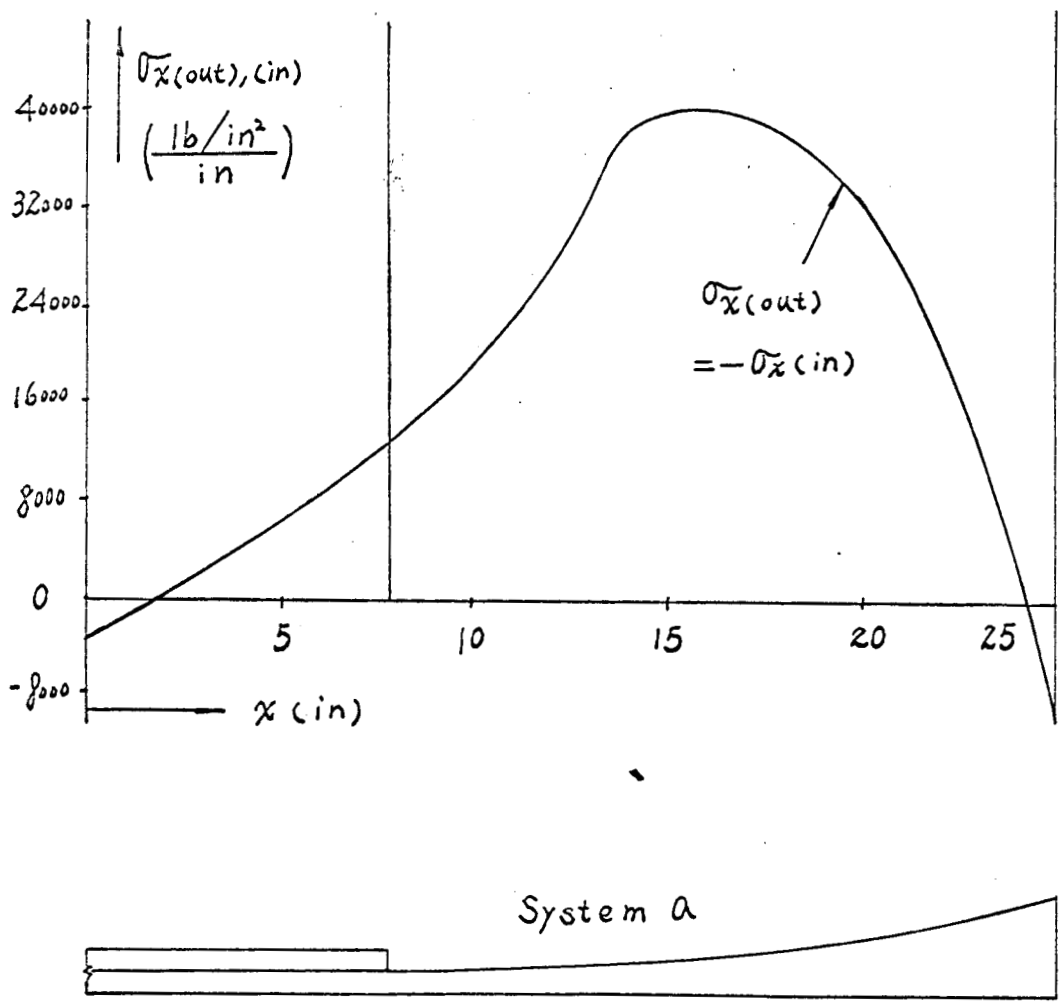

Fig. 25.--Resultant stresses in the upper cylindrical part for the illustrating temperature distribution

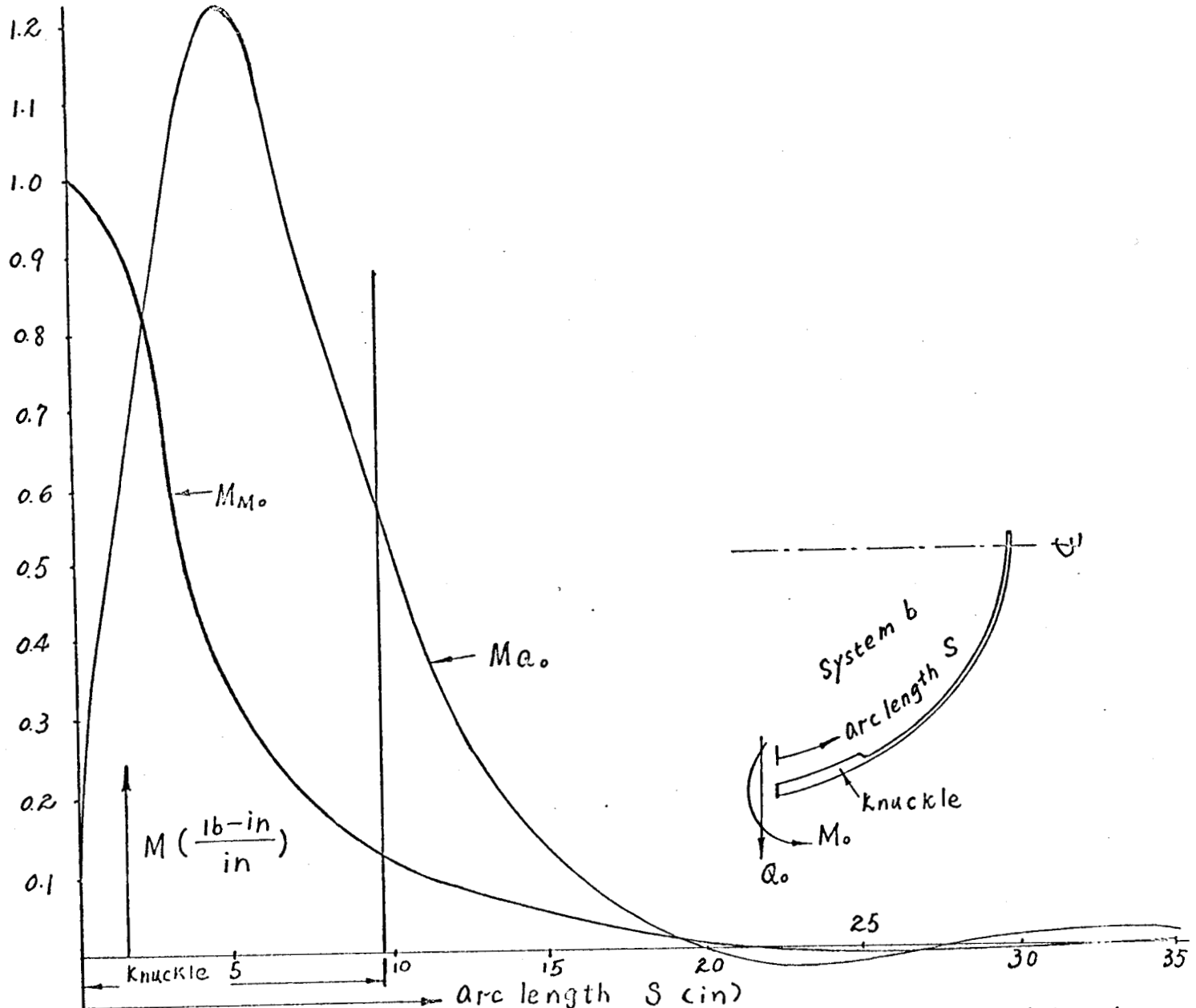

Fig. 26.--Meridional moment distribution in the bulkhead for $M_o = 1$ and $Q_o = 1$

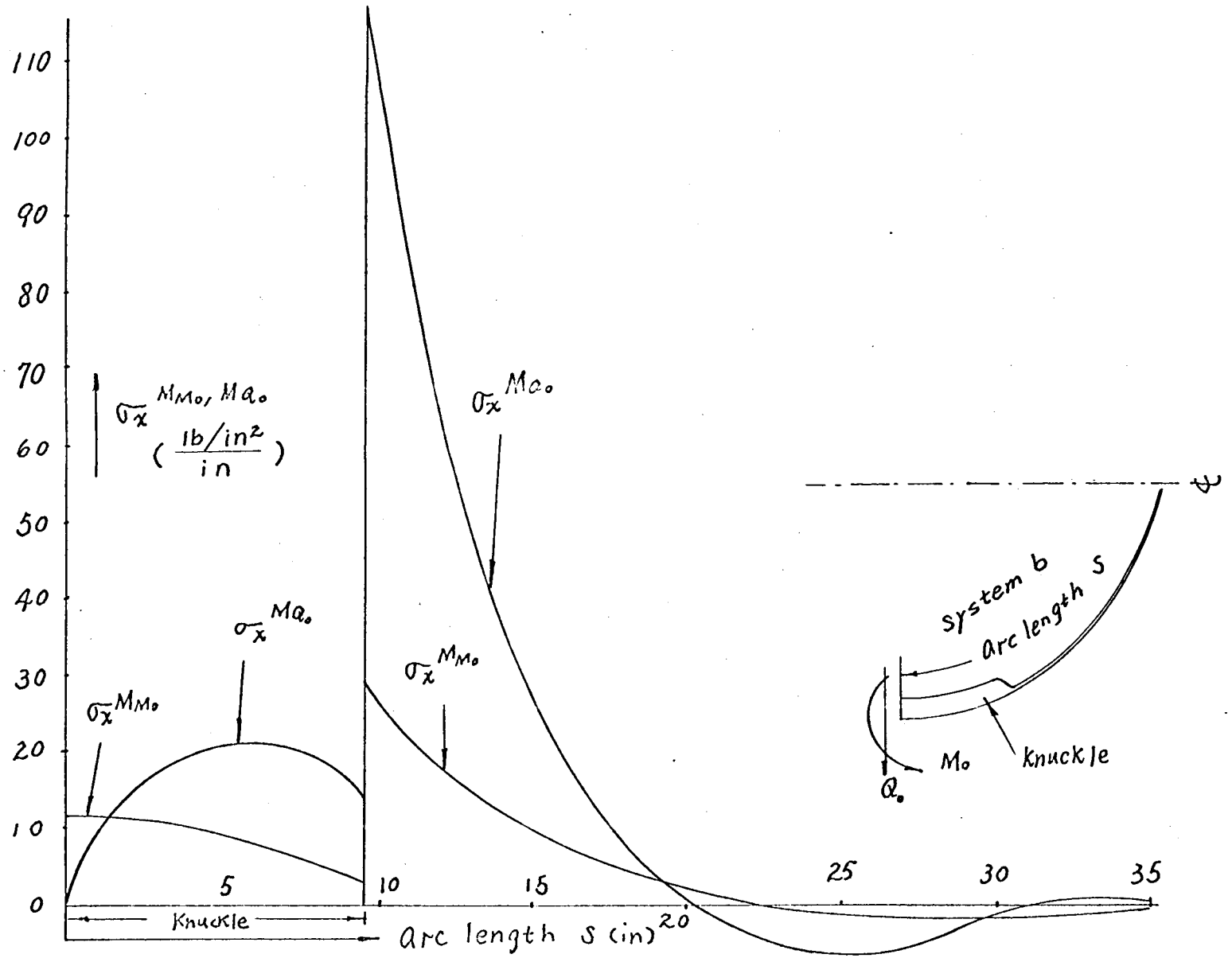

Fig. 27.--Bending stresses in the bulkhead for $M_o = 1$ and $Q_o = 1$

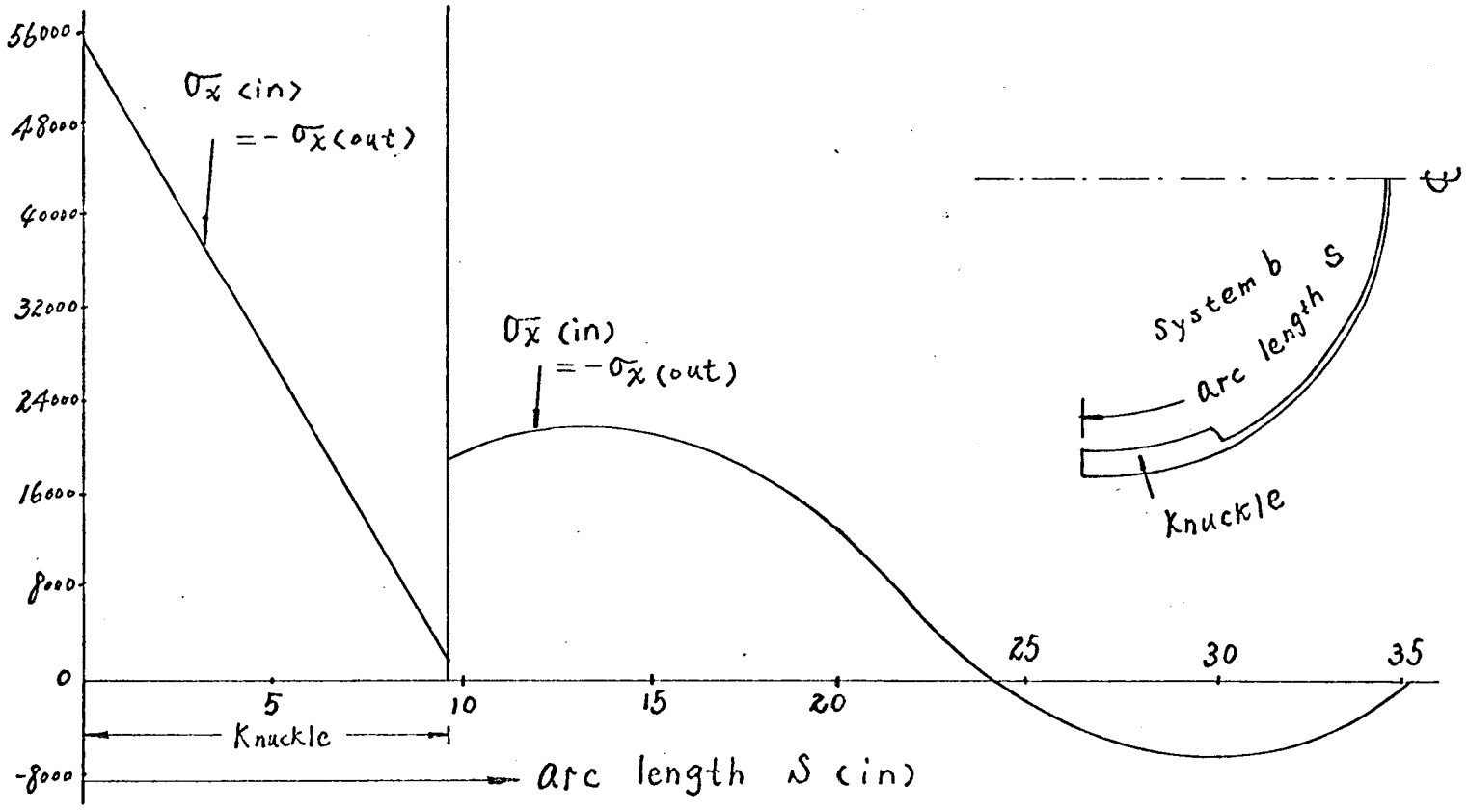

Fig. 28.--Resultant stresses in the bulkhead for the illustrating temperature distribution

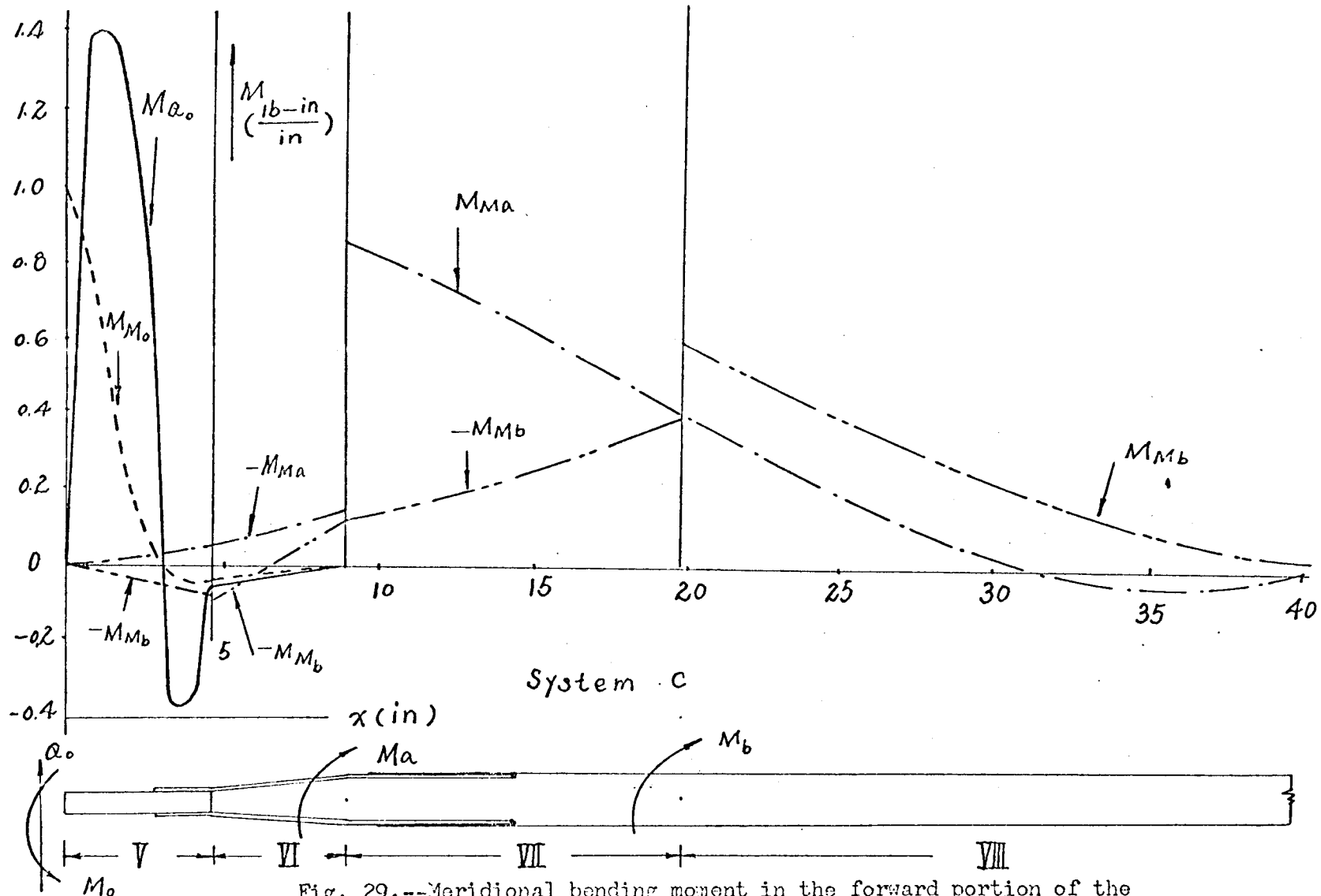

Fig. 29.--Meridional bending moment in the forward portion of the intertank skirt for $M_o = 1$, $Q_o = 1$, $M_a = 1$, $M_b = 1$

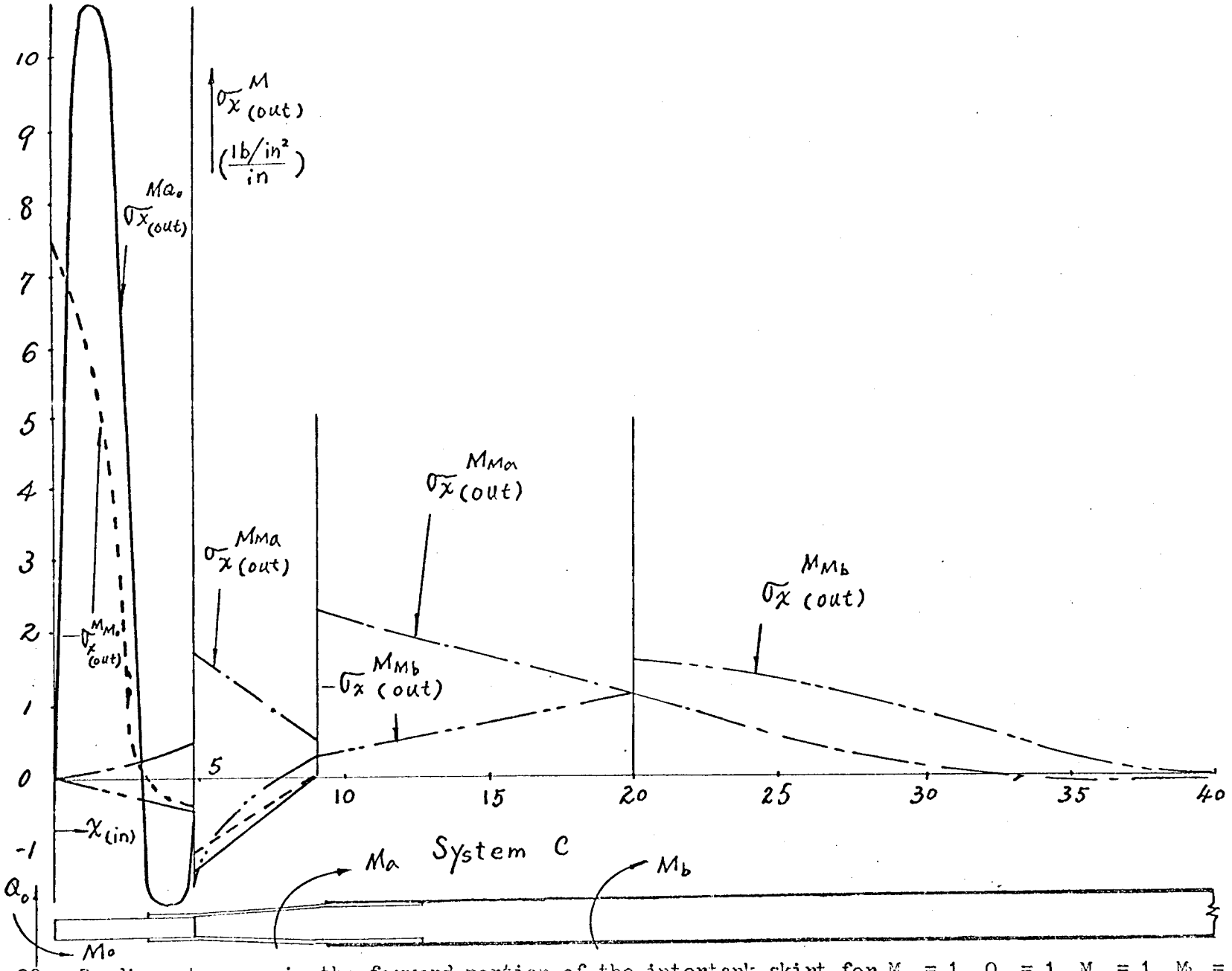

Fig. 30.--Bending stresses in the forward portion of the intertank skirt for $M_o = 1$, $Q_o = 1$, $M_a = 1$, $M_b = 1$

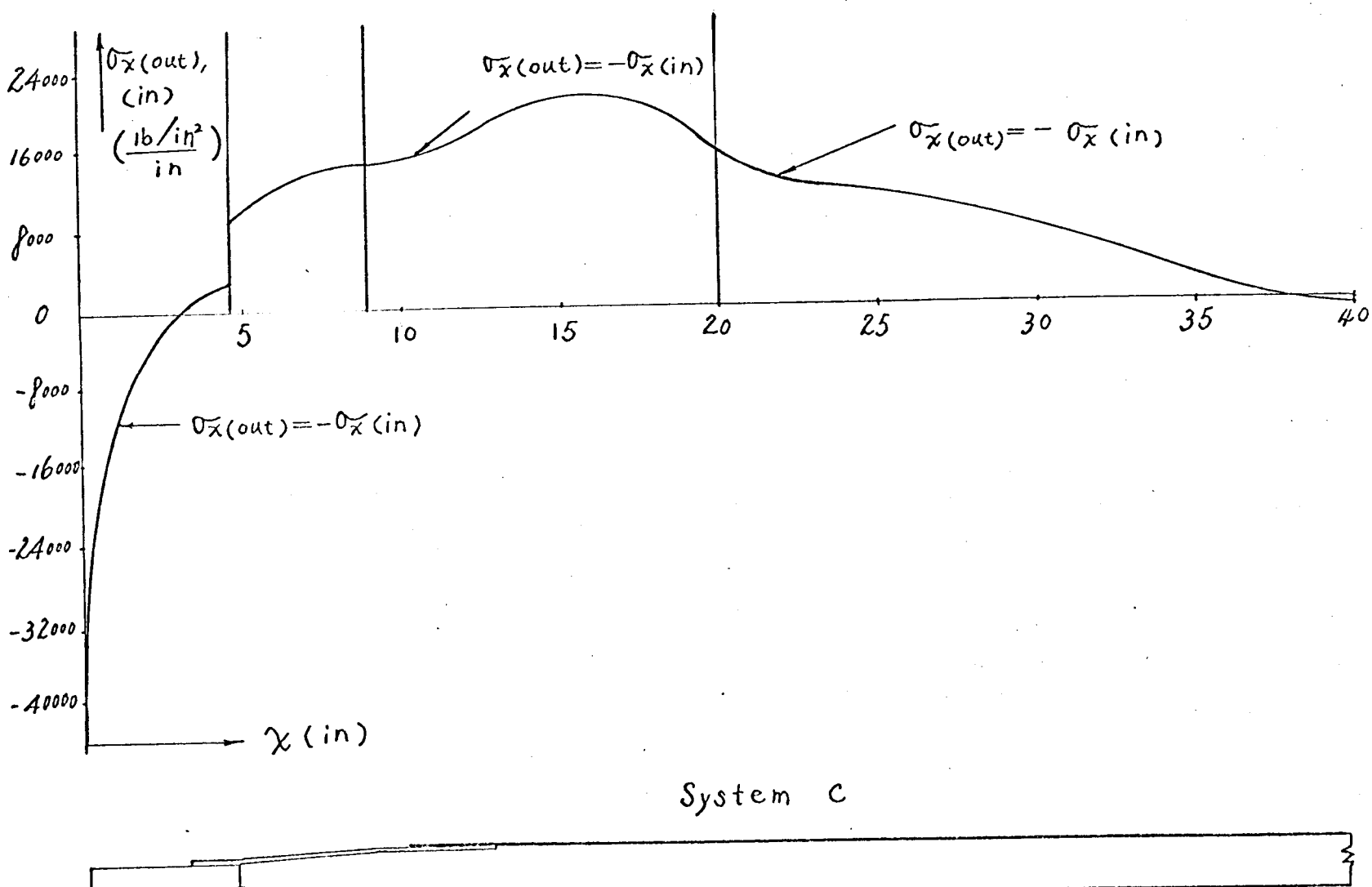

System C

Fig. 31.--Resultant stresses in the forward portion of the intertank skirt

CHAPTER V

DISCUSSION AND CONCLUSION

The theoretical analysis of the present work lies within the range of the linear theory of thin shells. This theory is based upon the assumption [10]

$$\text{Max}\frac{\delta}{R_2} \leq \frac{1}{20} \tag{161}$$

where δ is the wall thickness and R_2 the second principal radius of curvature of the middle surface.

The above ratio, as may be seen from the example of Chapter IV, is satisfied.

Due to the fact of large temperature variation, other assumptions such as the displacements at a point be small in comparison with the thickness of the shell is no longer as rigid as it should be. However, one has to bear in mind that the present temperature distribution may occur only in accompanying with the internal pressure loading. The effect of the latter diminishes the displacements obtained in the case of thermal loading. The linear assumption, as well as the theoretical analysis of the present investigation, is then valid for most problems in the same manner.

In our example, the boundary condition has been taken to be free of constraint at both ends. It will be, of course, sufficient in an analysis as far as the intertank as a whole is investigated independently.

The resultant stresses as shown in Figures 25, 28, and 31 have

not only the common points of maximum stresses with those from an investigation of the pressure loading, but also the final result, plotted as in Figure 28 shows that the thermal stresses considered in the present case have a release effect on the stresses from the pressure loading in the knuckle of the bulkhead. This is important, since the knuckle part will reach the yield point first for internal pressure.

APPENDIX

The displacement and rotation of the cantilever beam (Figure 14) may be obtained by considering the linearized theory of beams.

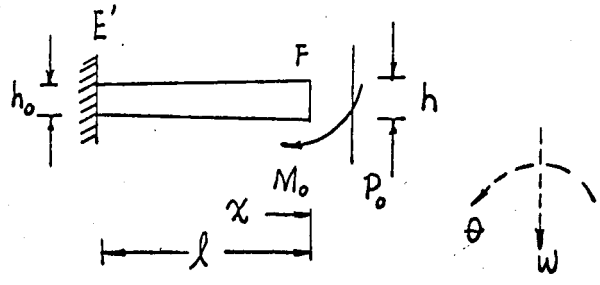

Fig. 32.--Part VI as cantilever beam

Let

h_o be thickness of the beam at E'.

h be thickness of the beam at F.

ℓ be length of the cantilever.

χ be horizontal axis, positive sense to the left with F as origin.

We have

$$\theta_\chi = \int_o^\chi \frac{M}{EI}\, d\chi + C_1 \tag{162}$$

(1) For $M_o = 0$

$$M = P_o \chi \,, \quad \text{and}$$

$$I = \frac{1}{12}\left[h - \frac{h-h_o}{\ell}\chi\right]^3 \tag{163}$$

equation (162) may be evaluated exactly.

$$\theta_x = \frac{12 P_o}{E\left(\frac{h-h_o}{l}\right)^2}\left[\frac{1}{h-\left(\frac{h-h_o}{l}\right)x} + \frac{h}{2\left(h-\frac{h-h_o}{l}x\right)^2}\right] + C_1 \qquad (164)$$

for $x = l$, $\theta = 0$

Let

$$\frac{h-h_o}{l} = a$$

we have

$$C_1 = \frac{12\ P_o}{E a^2 h_o}\left(1 - \frac{h}{2h_o}\right) \qquad (165)$$

and

$$\theta_x = \frac{12\ P_o}{E a^2}\left[\frac{1}{h_o}\left(1-\frac{h}{2h_o}\right) - \frac{1}{h-ax} + \frac{h}{2(h-ax)^2}\right] \qquad (166)$$

For the displacement

$$W_x = \int_o^x \int_o^x \left(\frac{M}{EI}\, dx\right) dx + C_2$$

$$= \int_o^x \theta_x\, dx + C_2 \qquad (167)$$

by substituting with (166), this may be evaluated

$$W_x = \frac{12\ P_o}{E a^2}\left[\frac{1}{h_o}\left(1-\frac{h}{2h_o}\right)x + \frac{1}{a}\log(h-ax)\right.$$

$$\left. + \frac{1}{a}\,\frac{h}{2(h-ax)}\right] + C_2 \qquad (168)$$

for $x = l$, $w = 0$

we have

$$C_2 = -\frac{12\,P_0}{E\,a^2}\left[\frac{1}{h_0}\left(1-\frac{h}{2h_0}\right)l + \frac{1}{a}\left(\log h_0 + \frac{h}{2h_0}\right)\right] \tag{169}$$

hence

$$W_x = \frac{12\,P_0}{E\,a^2}\left[\frac{1}{h_0}\left(1-\frac{h}{2h_0}\right)(x-l) + \frac{1}{a}\log\frac{h-ax}{h_0} + \frac{1}{a}\,\frac{h}{2}\left(\frac{1}{h-ax} - \frac{1}{h_0}\right)\right] \tag{170}$$

(2) For $P_0 = 0$,

$$M = M_0 \text{ , and}$$

$$I = \frac{1}{12}(h-ax)^3 \tag{171}$$

we have

$$\theta_x = \int_0^x \frac{M_0}{E\,I}\,dx + C_1$$

$$= \frac{M_0}{E}\int_0^x \frac{12}{(h-ax)^3}\,dx + C_1 \tag{172}$$

the integration may be carried out

$$\theta_x = \frac{6M_0}{E}\,\frac{1}{a}\,\frac{1}{(h-ax)^2} + C_1 \tag{173}$$

for $x = l$, $\theta = 0$

we have

$$C_1 = -\frac{6\,l\,M_0}{E(h-h_0)h_0} \tag{174}$$

hence

$$\theta_x = \frac{6 M_o l}{E(h-h_o)} \left[\frac{1}{(h-ax)^2} - \frac{1}{h_o} \right] \tag{175}$$

For the displacement

$$W_x = \int_0^x \theta_x \, dx + C_2 \tag{176}$$

by substituting with equation (175)

we have

$$W_x = \frac{6 l M_o}{E(h-h_o)} \left[\frac{l}{(h-ax)(h-h_o)} - \frac{1}{h_o} x \right] + C_2 \tag{177}$$

for $x = l$, $W = o$

we have

$$C_2 = - \frac{6 l M_o}{E(h-h_o)} \left[\frac{l}{h_o(h-h_o)} - \frac{l}{h_o} \right] \tag{178}$$

finally

$$W_x = \frac{6 l M_o}{E(h-h_o)} \left[\frac{l}{h-h_o} \left(\frac{1}{h-ax} - \frac{1}{h_o} \right) - \frac{1}{h_o} (x - l) \right] \tag{179}$$

LIST OF REFERENCES

1. "Beams on Elastic Foundation" M. Hetenyi, 1946, Oxford University.

2. "Advanced Strength of Materials" Part 1 and Part 2, S. Timoshenko, 1956, D. Van Nostrand Company, N. Y.

3. "Theory of Thermal Stresses" Bruno A. Boley and Jerome H. Weiner, 1960, Wiley & Son, N. Y.

4. "Thermal Buckling of Circular Cylindrical and Conical Thin-walled Shells" David Abir, 1958, Polytechnic Institute of Brooklyn.

5. "The State of Stress in Full Heads of Pressure Vessels" W. M. Coates, 1930, Journal of Applied Mechanics.

6. "Torispherical Shells--A Caution to Designers" G. D. Galletly, February, 1959, p. 51, Journal of Applied Mechanics.

7. "Structural Design of Missiles and Spacecraft" Lewis H. Abraham, 1962, McGraw-Hill, N. Y.

8. "Theory of Plates and Shells" S. Timoshenko, 1959, The Maple Press Company, York, Pa.

9. Work done in a related research work, Engineering Mechanics and Science Department, University of Florida, 1963, Gainesville, Florida.

10. "The Theory of Thin Shells" V. V. Novozhilov, 1959, Ove Arup & Partners, London.